Real-Time Monitoring of Short-Term Steel Corrosion in Cement and Soil

By

Shuvam Nandi

A thesis submitted to the Civil Engineering Department,

Cullen College of Engineering

In partial fulfillment of the requirements for the degree of

Master of Sciences

In Civil Engineering

Chair of Committee: Dr. Cumaraswamy Vipulanandan

Committee Member: Dr. Gino Lim

Committee Member: Dr. Y. Ling Mo

University of Houston

August 2021

ACKNOWLEDGMENTS

Before I proceed any further, I would like to add a few words of appreciation for the people who have been a part of this journey from its outset.

Firstly, I would like to express my greatest regards to my advisor and thesis committee chair, Dr. Cumaraswamy Vipulanandan, for his motivation, support, guidance, and suggestion for this research. I would also like to extend my sincere appreciation to committee members, Dr. Gino Lim and Dr. Y. Ling Mo for their insightful comments, encouragement, and time. I would also like to thank my Department Chair, Dr. Roberto Ballarini, for his support.

I would also like to thank Kripa Adhikari, Kopikah Tharmakulasingham, Sumnima Singh, Guru Panda, and Ahmed Aldughather for their valuable feedback and support throughout my research. I'd also like to thank our college coordinator, Ms. Miranda Vernon-Harrison for her help and guidance during my research. I thank all UH staff members for their support and kind help.

I am extremely humble towards my family who has given me the encouragement for anything I wanted to do throughout my academic perseverance. Lastly, I am thankful to all the faculty and staff members at the Department of Civil Engineering and Environmental Engineering at UH for teaching me something new every day.

ABSTRACT

The corrosion process is defined as an electrochemical reaction that causes the deterioration and loss of material which adversely affects the critical properties of a material such as its microstructure, mechanical properties, and physical appearance. Corrosion of steel is of particular interest as steel is the largest volume of metal used in the construction of most structures including buildings, bridges, storage facilities, and pipelines. Several testing methods have been used to detect and quantify corrosion such as visual inspection, weight-loss method, radiography, acoustic monitoring. However, most of these methods have limitations including field applications. In this study, the Vipulanandan Impedance Corrosion Model was used to assess and quantify the corrosion occurring in steel subjected to different environmental conditions. For this study, three different specimens were considered: (1) cement-steel casing immersed in 3.5 % saltwater for an observation period of 250 days, (2) steel bar in 10% moist sand for an observation period of 70 days, and (3) steel bar in 40% moist clay for an observation period of 70 days. The above steel specimens were allowed to corrode for the set observation period and the impedance data was collected from each specimen which was then used to get the model parameters: bulk resistance (Rb), contact resistance (Rc) & interface resistance (Ri), and contact capacitance (Cc) & interface capacitance (Ci) for the Vipulanandan Impedance Corrosion Model. The electrical corrosion index for each specimen was then observed over time to understand the corrosion mechanism.

TABLE OF CONTENTS

LIST OF TABLES

LIST OF FIGURES

CHAPTER 1 INTRODUCTION

1.1 General

Most civil engineering structures use metal including steel as construction material. All structures, whether built above the ground such as buildings, bridges, and roads or those built underground such as foundations, basements, and pipelines, all require the use of metallic structural components. One of the main concerns regarding the service life of such structures is corrosion. It is very important to consider corrosion as a parameter when designing such structures as it may not only affect the structural performance in the long run but also because of its economic impact.

It has been seen that the costs attributed to corrosion damages of all kinds are estimated to be 3% to 5% of industrialized countries' gross national product (Schütze, 2002). In the United States, many government studies have shown that the cost due to corrosion loss is almost $300 billion annually (*Corrosion: Understanding the Basics (March 19, 2000)*, 2021). The loss of material by corrosion is a waste not only of the steel structures, but also of the energy, water, and human effort that was used to produce and construct the structures. In addition, the replacement of the corroded steel structures requires the further investment of all these resources (Secer et al, 2016).

In the present study evaluation of corrosion in real-time is of utmost importance. Using the Vipulanandan Impedance Corrosion Model the quantification of corrosion in steel subjected to different environmental conditions has been studied.

1.2 Problem Statement

Several methods have been used by researchers to evaluate the damage dealt with structures by corrosion. Some of these include visual inspection, weight loss measurements, radiography, ultrasonic and acoustic testing, liquid penetration and leak detection methods, and electrical methods. Most of these methods require a substantial amount of time for precise detection and

measurement. Additionally, most of these methods require lab testing. But in situations where it is impossible to obtain lab samples or in places where the test setup cannot be reached it is impossible to utilize these methods. It is therefore vital to make use of nondestructive testing methods (NDT) for in situ corrosion measurements which not only provide data fast but also precisely. Most of the issues that are encountered using the above methods can easily be tackled by using Electrochemical processes to evaluate the extent of damage to the metal in corrosive media. Various electrochemical procedures like the Linear Polarization Resistance (LPR) process, Electrochemical Impedance Spectroscopy (EIS) procedure, and Electrochemical Noise measurements are accustomed to monitoring the corrosion rate of the metallic surface.

1.3 Objective

The overall objective of the research study was to use the Vipulanandan Impedance Corrosion Model to quantify the corrosion occurring in steel specimens when placed in different media. Specific objectives include the following:

1. Investigate the effect of moisture content on the critical electrical resistivity of soil.
2. Identify the equivalent electrical circuit needed to model the electrical resistance data for the steel corrosion specimens.
3. Quantify the corrosion occurring in cement-steel casing immersed in 3.5% salt solution.
4. Quantify the corrosion occurring in steel bar placed in 10% moist sand and 40% moist clay.

1.4 Organization

This thesis is organized into seven chapters. Chapter 1 is the introduction to this research study, which presents the research problem that was the focus of this study, in a detailed manner. Chapter 2 summarizes the background and literature review related to the corrosion process in structures. In chapter 3, materials used for preparing the corrosion specimens are discussed. It also provides the necessary theory and information about the testing method used and modeling of the electrical resistance data of the corrosion specimens. Chapter 4 discusses the effect of moisture

content on the electrical resistivity of soil. Corrosion study on cement-steel casing immersed in saltwater is presented in chapter 5 followed by the corrosion study of steel bar in moist soil conditions in chapter 6. Finally, the major findings of this research have been summarized in Chapter 7.

CHAPTER 2 BACKGROUND AND LITERATURE REVIEW

2.1 Introduction

The main purpose of this chapter is to provide a review of the topics that are closely related to the proposed study. This chapter summarizes the corrosion process in structures, some of the major accidents that have occurred in structures due to corrosion as well as past research on the factors that affect the corrosion process in buried structures. A review of the methods used to assess corrosion in buried structures is also presented in this chapter.

2.2 Corrosion in Structures

The corrosion process can be defined as an electrochemical reaction that causes the deterioration and loss of material which adversely affects the critical properties of a material such as its microstructure, mechanical properties, and physical appearance. For example, steel on corrosion loses its strength and changes in appearance. Corrosion is a widespread problem that affects all underground structures. The failure of such structures due to corrosion has several consequences on the environment, the economy as well as human life (Ekine, 2010). Most incidents that involve corrosion go unnoticed. This could be because of human liability or the disappearance of useful evidence in the aftermath (Mazumder, 2020). However, some incidents have been highlighted throughout history. A list of some of the accidents that have occurred throughout history due to corrosion is summarized in Table 2-1.

Table 2-1 Accidents due to corrosion

Name of the Accident	Year	Location	Infrastructure	Reasons for Failure	Remarks
Silver Bridge Accident	1967	Ohio, USA (offshore)	Highway bridge	Stress corrosion and corrosion fatigue	1. A minute crack formed during casting 2. Technology not advanced to detect cracks at the time

Table 2-1 continued

Bhopal Gas Tragedy	1984	Bhopal, India	Chemical storage tanks	Corroded pipes, valves and other safety equipment	Negligence of deterioration of safety standards and maintenance procedures at the plant
Swimming Pool Roof Collapse	1985	Uster, Switzerland	Concrete roof	Chloride induced stress corrosion cracking	Failure to detect high traces of chlorine gas in the atmosphere of the building
Aloha Airlines Flight 243	1988	Island of Maui, Hawaii	Upper fuselage of passenger airplane	Multiple corrosion induced fatigue damage	Failure to detect corrosion damage
Guadalajara Sewer Explosion	1992	Guadalajara, Mexico	Sewer	Leakage of gasoline into sewer from a corroded gasoline pipeline	1. Despite several complaints no investigation was carried out by local authorities 2. Damage costs estimated 75 million U.S. dollars
Gaylord Chemical Explosion	1995	Louisiana, USA	Railroad tank car	Contamination of nitrogen tetroxide with water, resulting in the formation of corrosive product which caused failure of tank	Lack of adequate procedures to prevent or detect the contamination of nitrogen tetroxide with water which resulted in the formation of extremely corrosive product
Sinking of Erica	1999	Brittany, France (Offshore)	Oil tanker	High corrosion damage to several parts	Negligence of severe corrosion damage that had already occurred

Table 2-1 continued

Carlsbad Pipeline Explosion	2000	New Mexico, USA	Natural gas pipeline	Severe internal corrosion by microbial activity	1. Failure to detect microbial activity in pipes. 2. All four types of microbes (sulphate reducing, acid producing, aerobic and anaerobic) were found in the pits formed in the pipes
Mihama Nuclear Power Plant Accident	2004	Mihama, Japan	Nuclear Power Plant	Rupture of carbon steel pipe carrying high pressure high temperature steam caused by flow accelerated corrosion	Fault assessment of pipe sections affected by wall thickness degradation should have been made a priority
Prudhoe Bay Oil Spill	2006	Alaska, USA	Pipeline	Failure of field pipeline due to lack of proper corrosion monitoring	1. Inadequate corrosion monitoring 2. Insufficient level of corrosion inhibitor liquid in pipeline

2.3 Factors Affecting Corrosion of Buried Structures

Corrosion of buried metal structures depends on various characteristics of the soil in which they are buried. Some of the well-known parameters that may affect the corrosion process are soil texture, soil moisture content, redox potential, pH, electrical resistivity, and ionic content (Arriba-Rodriguez et al, 2018). These are summarized as follows:

2.3.1 Soil Texture:

Soil texture comprises the proportion of sand, silt, and clay particles that make up the fraction of the soil. Depending on the proportions of the sand, silt, and clay particles present in the soil, the soil may be categorized as per the soil texture triangle shown in Figure 2-1. The soil texture influences the water holding capacity as well as the water flow through the soil. For example, clay

is poorly aerated and has a high-water holding capacity. In contrast, sand has a very high aeration degree but has a very low to no water holding capacity. The corrosivity of soil may also be influenced by the soil texture. Particle fineness also affects the corrosivity of the soil. It has been seen that clay, having a high mineral content, absorbs more water due to its higher surface area and is, therefore, more corrosive towards buried metal structures.

2.3.2 Moisture Content

Moisture content is an important parameter to assess the corrosivity of soil. It plays a major role in the corrosion process of buried metal structures. It acts as the necessary electrolyte for the electrochemical corrosion reactions to take place. Several studies have shown a direct relationship between the moisture content of the soil and corrosion rate. Gupta and Gupta (1979) performed a series of laboratory experiments in which steel specimens were buried at different locations in India. Each location had different

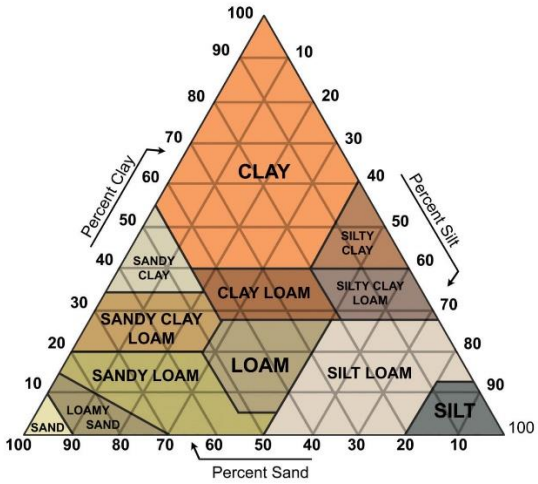

Figure 2-1 Soil Texture Triangle

soil properties in comparison to the other locations. The soil types were sand, sandy loam, and loam. From this study, a strong correlation was found between mass loss and moisture content. It was found that mass loss increased with increasing moisture content up to an intermediate moisture

content level beyond which there was no further increase in the mass loss. This intermediate moisture content was termed as the critical moisture content. In another study, Noor-Al-Moubaraki (2014) studied the effect of moisture content on the corrosion behavior of X60 steel. Samples were buried in soils from different cities in Saudi Arabia at an ambient temperature of 29±1°C. It was observed that the corrosion rate increased with increasing moisture content up to a maximum value of 10% beyond which it decreased. Ezuber et al. (2020) also carried out a study to assess the effect of soil texture and moisture content on the corrosion process of mild steel specimens. They found that the severity of the underground steel corrosion varied with moisture content. The maximum corrosion occurred when the moisture content was between 20 and 25% (by weight). These studies show the dependence of corrosion of buried metal structures on the moisture content of the soil. It also confirms the presence of critical moisture content at which maximum corrosion rate can be observed. This critical moisture content varies from soil to soil.

2.3.3 Redox Potential

Redox potential is a measure of the degree of aeration of the soil and can be used as an indicator of soil corrosivity (Veleva, 1996). It is calculated from the potential difference measured with a probe that contains an inert platinum (Pt) electrode and a saturated calomel electrode (Hg/Hg2Cl2/KCl, +0.241 V versus Standard Hydrogen Electrode (SHE)) as a reference electrode. The value of the soil's redox potential depends on the dissolved oxygen present in the pore water and provides some information on the conditions under which sulfate-reducing bacteria could grow. The use of redox potential to predict the soil's corrosivity is shown in Table 2-3.

Table 2-2 Soil redox potentials as an indicator for soil corrosivity (Veleva, 1996)

Redox Potential (vs SHE)	Aeration	Soil Corrosivity Category
Negative	Not aerated	Extremely severe
0 – 100 mV	None to weak	Severe

Table 2-2 continued

100 – 200 mV	Weakly aerated	Moderate
200 – 400 mV	Aerated	Slight
Above 400 mV	Strongly aerated	Non-corrosive

2.3.4 pH

The pH of the soil was considered as the factor most affecting the underground corrosion since its discovery. Researchers working in the field of underground corrosion tried to relate the pH of the soil to a high corrosion rate. Romanoff (1957) conducted comprehensive field investigations for 25 years to relate the pH of soil and corrosion rate of pipes between the years of 1922 and 1952 in the United States. Thousands of metal specimens were buried underground at different locations across the US; the pH of the soil was measured at each location. A correlation between the long-term mass loss and pH of the soil was established. Penhale (1984) buried steel plates at thirty-three different locations with varying soil types for 20 years. For each soil, the pH and the total acidity were measured. No correlation could be found between the pH and the corrosion rates. Rajani and Makar (2000) examined the corrosion rates of cast iron pipes obtained under various pH conditions of pipes. Based on their data, no correlation was observed between pH and pitting rates. Doyle et al. (2003) compared the results of pH testing with the corrosion rates of samples from 98 selected sites in Ontario, Canada, and found no correlation between pH and corrosion rates. He too found no ($R^2 = 0.04$) correlation between pH and corrosion rate. Apart from some of the early works no other author has found any positive correlation between pH and corrosion rate of buried pipes. It can be said that a low pH soil could be used as an inference for the occurrence of corrosion; however, there are many other contributing factors towards the corrosion of buried pipes in soil. To conclude, there is no ascertained correlation between the pH of the soil and the corrosion rate of buried pipes ().

2.3.5 Electrical Resistivity

Soil electrical resistivity is one of the main factors that are closely related to corrosion in soil. The electrical resistivity of a substance is a measure of its ability to resist/conduct the flow of electric current through it (McNeil, 1980). In soil, the electrical resistivity varies with depth and width due to changes in the soil composition, moisture content, and temperature. With increasing moisture content, electrical resistivity decreases to a certain minimum value. The presence of soluble salts in the soil also reduces the electrical resistivity of the soil (Lim et al, 2013). Particle size also affects the resistivity value of the soil. For example, sandy soils with their relatively large particle size offer better aeration and therefore allow for quicker drainage and evaporation of moisture than clayey soils. Hence, sandy soils have a higher resistivity value often in the range of a few hundred to thousand ohm-meters and therefore are considered less corrosive. Clayey and silty soils with resistivities in the range of 5 to 20 ohm-meters are corrosive. This is likely since they have a higher water retention capacity than other soil types. The resistivity of clay and silt is largely dependent on the available moisture content and, therefore, dry clay and silt, in theory, have a higher resistivity. It is therefore important to consider soil resistivity and its variation with change in moisture content and temperature when designing underground pipelines and other similar structures. The lower value of resistivity can worsen the corrosion on the outer surface of the pipelines and as a result, additional costs may have to be borne for the application of the suitable protective coating on the outer surface before laying them underground.

2.3.6 Ionic Content

The main chemical components that are primarily known to be responsible for corrosion reactions are chlorides and sulfates. Chloride ions can be harmful as they participate directly in the reaction of the anodic dissolution of metals. They are also responsible for reducing the resistivity of the soil. According to a study done by Song et al (2017) low levels of chloride ions tend to cause general corrosion while high levels of chloride may likely induce localized corrosion. Higher

concentrations of chloride ions in the soil induce higher corrosion rates, larger pit depths and suppress the decreasing corrosion rates, especially during the initial phase. After longer exposure periods, however, the higher concentration of chloride ions may thicken the rust layers thus impeding the corrosion process. Chloride ions may be present naturally in the soil as a result of brackish groundwater or may enter through external means like deicing salts applied to roads during winter. Chloride ion concentration also varies depending on the moisture content of the soil (Ismail, 2009). In comparison to chlorides, the effect of sulfates on the corrosion process is rather low. However, the risk increases when sulfates get converted to corrosive sulfides due to anaerobic sulfate-reducing bacteria.

2.4 Methods to Evaluate Corrosion

2.4.1 Qualitative Methods

The qualitative methods use certain parameters, that directly or indirectly affect corrosion, to estimate the corrosion potential of the soil in which steel is buried. In this method the more the number of parameters the model considers, the more is the reliability of the model's estimation of the corrosion potential of the soil. The main advantage of using these methods is that they usually make use of tables or diagrams that are rather easy to understand. The main disadvantage of the qualitative methods is that while they can be used to estimate how likely the corrosion of a certain buried metal is to occur it does not provide a numerical value.

Over the passing years, as corrosion began to be recognized as a pressing concern to engineering structures, several qualitative methods came into emergence. At first, scientists tried to use a univariate approach in which they considered only a single parameter, which they believed to have the most significant effect on the degradation of the structure, in their models to estimate the corrosion potential of the soil. The National Association of Corrosion Engineers (NACE) and the American Society for Testing and Materials (ASTM) put forward tables that related the resistivity

of the soils to the degree of corrosion. In 1946, Starkey and Wight developed a model that related the corrosion potential of the soil to the redox potential of the soil. Other researchers tried to associate the corrosivity potential of the soil with the pH of the water extract of the soil. However, in time researchers came to realize that the corrosion mechanism in buried structures is not dependent on the only one said parameter and that it was dangerous to just consider the effect of only one. Thus, researchers began to develop models that made use of a multivariate approach. In 1963, Pourbaix used pH and potential to represent the corrosion mechanism in the form of diagrams called Potential-pH diagrams. Another model to estimate the corrosion was developed in the European standard EN 12501-2:2003. This model used pH and resistivity as its two parameters for modeling. The American Water Works Association (AWWA) also developed a multivariate approach based on a point scale known as the soil corrosivity scale. In this method of approach, the most important parameters in the corrosion process are assigned a score based on the characteristics of the soil in which the metal structure will be buried. Each parameter is also assigned a different weight depending on its rate of affection to corrosion. As opposed to previous multivariate approaches, here not only multiple parameters are considered but each parameter's effect and severity towards the corrosion process is considered.

2.4.2 Quantitative Methods

Qualitative methods are those methods of assessment that provide a numerical value to the corrosion. Most of the quantitative methods involve collecting field data which enables the engineer to design the structures according to the useful life required by each project.

Romanoff was the first scientist who revolutionized the field of underground corrosion. The research carried out by Romanoff involved burying several pieces of different grades of steel in soils for long periods, from months to several years, to understand how the corrosive soil affected the different steel. In his study that lasted for 20 years, he tried to determine if the soil properties could be used to predict corrosion. To test the applicability of the results of his study, he selected

various soils with different characteristics. The soils were analyzed to determine their physical, chemical, grain size, and climatic characteristics. At each location, several samples of steel, both bare and coated, were buried. The samples were periodically recovered and taken to a laboratory where the mass loss was evaluated. Due to his efforts, it was possible to evaluate the behavior of corrosion in steel in the soil for different periods. In 1988, the National Bureau of Standards (NBS) became the National Institute of Standards and Technology (NIST) and published a study titled: "Analysis of Pipeline Steel Corrosion Data from NBS Studies Conducted between 1922 to 1940 and Relevance to Pipeline Management", with a detailed analysis of the information given by Romanoff's studies.

2.5 Summary

Based on the literature review related to corrosion of structures, factors affecting corrosion process, and methods used to evaluate corrosion, the following can be summarized:

1. Corrosion is an electrochemical reaction that causes the deterioration of and loss of material which in turn has adverse effects on the material's properties.
2. Over the years several accidents have occurred due to corrosion in structures. Most of these accidents have occurred due to the lack of proper knowledge as well as the lack of any method to monitor the corrosion process.
3. Corrosion of underground structures depends on several factors including soil texture, moisture content, redox potential, pH, electrical resistivity, and ionic content.
4. Two different types of methods for assessing corrosion have been discussed: qualitative methods and quantitative methods. Qualitative methods make use of parameters that directly or indirectly affect corrosion to estimate the corrosion potential of the soil in which the structures are buried. Quantitative methods on the other hand provide a numerical value concerning the corrosion in the structure.

CHAPTER 3 MATERIALS AND METHODS

3.1 Introduction

This chapter has been divided into two parts: (1) Soil studies and (2) Corrosion studies. In the first part of the study, the effect of moisture content on the electrical resistivity of soil has been discussed. The resistivity value of the soil specimens is also compared to standard X to check their corrosivity rating. This is followed by the investigation and quantification of corrosion in the following three case studies: (1) corrosion of cement-steel casing immersed in 3.5 % NaCl solution, (2) corrosion of steel bar in moist sand and clay, and (3) corrosion of steel bar in saline sand and clay. The detailed procedure to prepare each sample and the tests performed on it has been discussed below.

3.2 Preparation of Specimen for Soil Studies

A cylindrical mold 4 inches in height and 2 inches in diameter was used. Three insertions were made on the curved surface of the mold, two of them on one side and the third on the diametrically opposite side, for the wire probes to be inserted. Figure 3-1 shows the pictorial representation of the experimental setup for electrical measurements. Two soils were used for the study: Ottawa sand and bentonite clay. Tap water was used as the essential electrolyte. A total of four specimens were prepared with varying moisture contents. In the case of sand four different moisture contents were used: 5%, 10%, 15%, and 20% while in the case of bentonite clay they were: 10%, 20%, 30%, and 40%. For each increment in the moisture content of the specimens, their weight was recorded followed by measurement of the resistance and reactance values using a commercial LCR device over a frequency sweep ranging from 20 Hz to 300 kHz. For this experiment, readings were noted at the following frequencies: 20 Hz, 40 Hz, 60 Hz, 80 Hz, 100 Hz, 500 Hz, 1 kHz, 5kHz, 10 kHz, 50 kHz, 100 kHz, 150 kHz, 200 kHz, 250 kHz, and 300 kHz. A soil conductivity meter was used to measure the conductivity of the specimen. To get the resistivity value, the reciprocal of the conductivity value was taken.

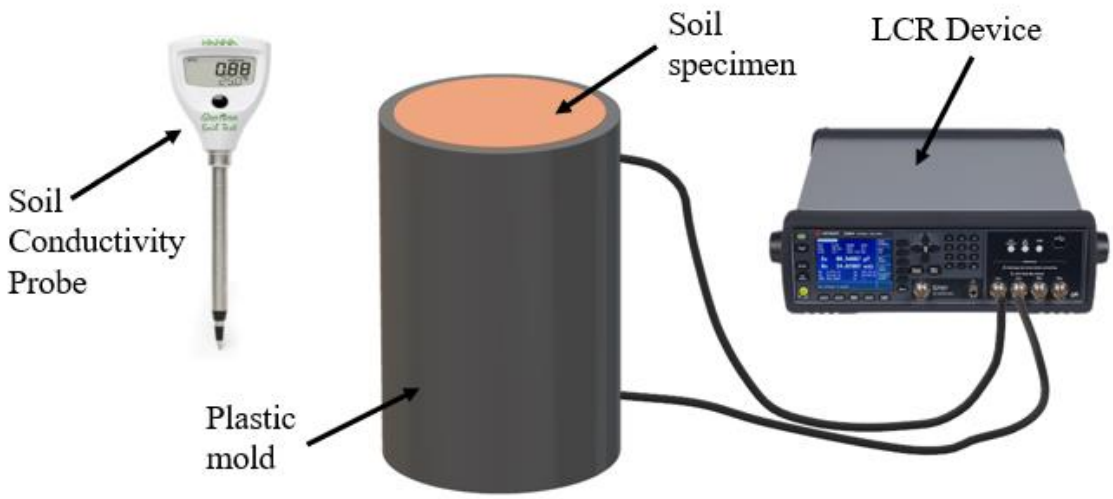

Figure 3-1 Setup of soil specimen for electrical resistance and resistivity measurements

3.3 Preparation of Specimen for Corrosion Studies

3.3.1 Cement-steel casing immersed in 3.5% NaCl solution

The specimen was prepared using a cylindrical mold of diameter 4 inches and height 4 inches. Circular cutouts of diameter 2 inches were made on the top and bottom surfaces of the mold for the steel pipe to pass through. Four insertions were made on the sides of the mold, two on either side, to allow the wire probes to be inserted into the cement. The pictorial representation of the cement-steel casing is shown in Figure 3-2. The cement slurry was prepared using a water-to-cement ratio of 0.4. Commercially available oil well cement (Class-H cement) and tap water were used. The mixing method adopted was hand mixing. On demolding the specimen after one day, the specimen was placed inside a bucket containing 3.5 percent salinity NaCl solution. The electrical resistance readings of the specimen were monitored using a commercial LCR device for 250 days.

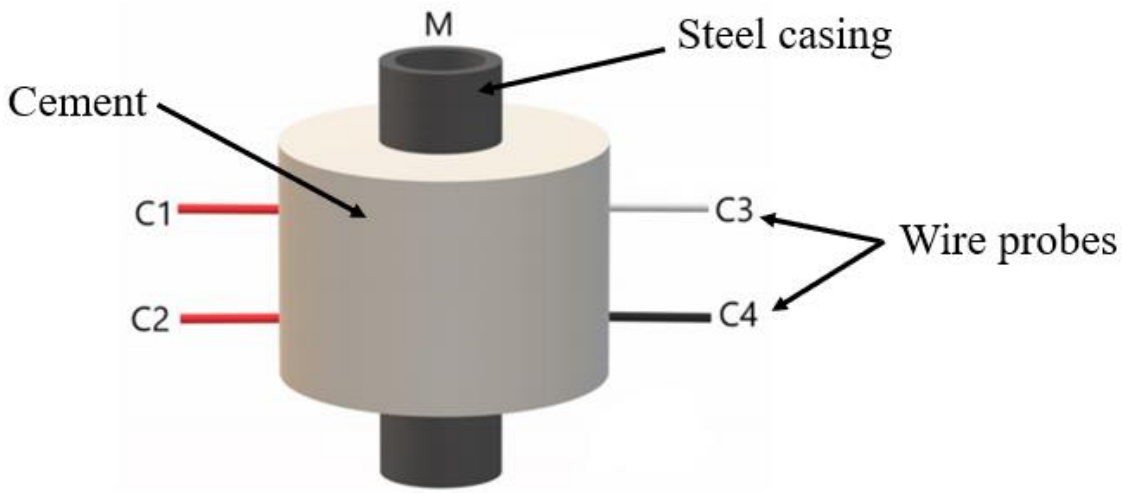

Figure 3-2 Probe configuration for electrical resistance measurements of cement-steel casing

3.3.2 Steel bar in moist soil

A cylindrical mold of height 4 inches and diameter 4 inches was used, like the one used in the cement-steel casing specimen. Four insertions were made, two on each side of the mold, for the wire probes to pass through. A bottom cutout was made for the steel bar to go through. The pictorial representation of the specimen with the probe configurations is shown in Figure 3-3. The steel bar has initial dimensions of 15 cm x 2.5 cm x 0.5 cm with a density of 7.53 g/cm^3. Two specimens were made: one with Ottawa sand with 10 % moisture content and the other with bentonite clay with 40% moisture content. The weight of the specimens was recorded followed by measurement of the resistance and reactance values using a commercial LCR device over the frequency range of 20 Hz to 300 kHz. The electrical measurements were taken for 11 different wire probe configurations: 6 combinations for both contacts with moist sand, 4 combinations for one contact with moist sand and the other to the steel bar, and 1 combination for both contacts made to the two ends of the steel bar.

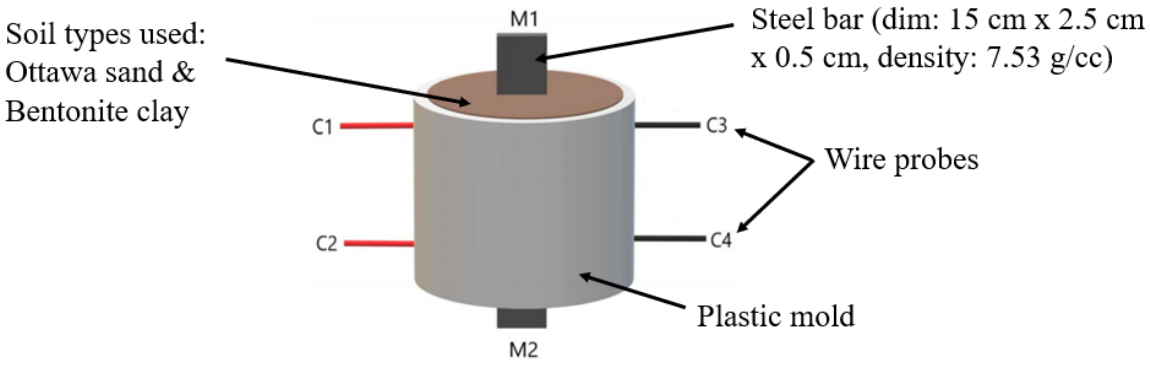

Figure 3-3 Probe configuration for electrical resistance measurements of steel bar in the moist soil specimen

3.4 Vipulanandan Impedance model for corrosion modeling

3.4.1 Equivalent circuit

To understand the properties of the material it is important to identify the most appropriate equivalent circuit to represent the electrical properties of the material. In this study, an equivalent circuit to represent the surface and bulk corrosion were required for better characterization through the analyses of the impedance spectroscopy data (Vipulanandan et al, 2013-2015). It was necessary to link the different elements in the circuit and the different regions in the impedance data of the corresponding sample. Given the difficulties and uncertainties, researchers tend to use a pragmatic approach and adopt a circuit which they believe to be most appropriate from their knowledge of the expected behavior of the material under study and demonstrate that the results are consistent with the circuit used. Two different possible equivalent circuits were analyzed to find an appropriate equivalent circuit to represent the two cases under study – (1) cement-steel casing in 3.5% NaCl solution and (2) steel bar in moist soil.

3.4.2 Case 1: General Bulk material – Resistance and Capacitance

In the equivalent circuit for Case 1, the contacts were connected in series, and both the contacts and the bulk material were represented using a capacitor and a resistor connected in parallel (Figure 3-4).

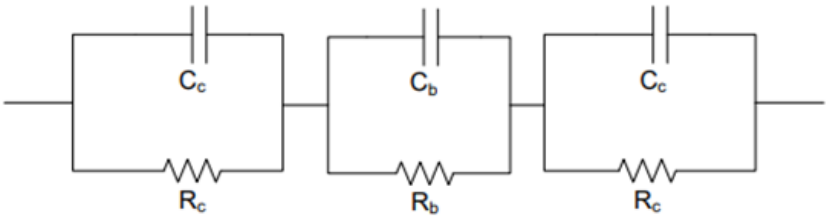

Figure 3-4 Equivalent circuit for Case 1

In the equivalent circuit for Case 1, R_b and C_b are the resistance and capacitance of the bulk material, respectively and R_c and C_c are the resistance and capacitance of the contacts, respectively. Both the contacts are represented with the same resistance (R_c) and capacitance (C_c) as they are identical. The total impedance of the equivalent circuit for Case 1 can be represented as

$$Z_1 = \frac{R_b}{1+\omega^2 {R_b}^2 {C_b}^2} + \frac{2R_c}{1+\omega^2 {R_c}^2 {C_c}^2} - j\left\{\frac{\omega {R_b}^2 C_b}{1+\omega^2 {R_b}^2 {C_b}^2} + \frac{2\omega {R_c}^2 C_c}{1+\omega^2 {R_c}^2 {C_c}^2}\right\} \qquad (3-1)$$

where ω is the angular frequency of the applied signal. When the frequency of the applied signal is very low, $\omega \to 0$, $Z_1 = R_b + 2R_c$, and when it is very high, $\omega \to \infty$, $Z_1 = 0$.

3.4.3 Case 2: Special Bulk material – Resistance only

Case 2 is considered as a special case of case 1 in which the capacitance of the bulk material (C_b) is assumed to be negligible (Figure 3-5).

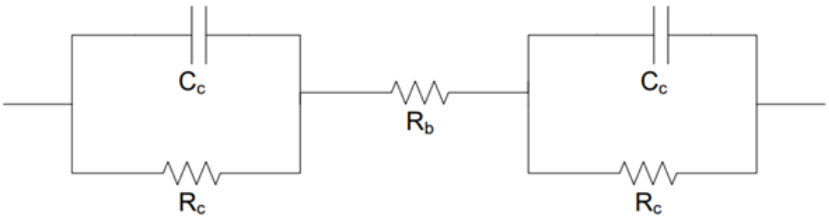

Figure 3-5 Equivalent circuit for Case 2

The total impedance of the equivalent circuit for Case 2 (Z_2) is

$$Z_2 = R_b + \frac{2R_c}{1+\omega^2 {R_c}^2 {C_c}^2} - j\left\{\frac{2\omega {R_c}^2 C_c}{1+\omega^2 {R_c}^2 {C_c}^2}\right\}. \qquad (3-2)$$

When the frequency of the applied signal is very low, $\omega \to 0$, $Z_2 = R_b + 2R_c$, and when it is very high, $\omega \to \infty$, $Z_2 = R_b$. In the case of corrosion measurement, the two contacts will have different properties and will be represented as shown in Figure 3-6.

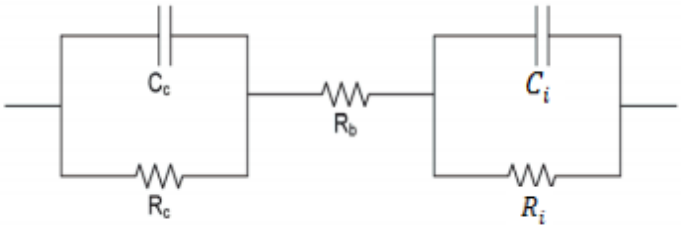

Figure 3-6 Vipulanandan Impedance Corrosion Model for Two Probe Measurements

Case 2 equivalent circuit was used to determine the contact electrical resistance (R_c) and contact capacitance (C_c) at the surface between the cement and the probe. During the impedance characterization, 15 data points were collected during each test and the data was used to determine the five unknowns in

$$Z = R_b + \frac{R_c}{1+\omega^2 {R_c}^2 {C_c}^2} + \frac{R_i}{1+\omega^2 {R_i}^2 {C_i}^2} - j\left\{\frac{\omega {R_c}^2 C_c}{1+\omega^2 {R_c}^2 {C_c}^2} + \frac{\omega {R_i}^2 C_i}{1+\omega^2 {R_i}^2 {C_i}^2}\right\}. \qquad (3-3)$$

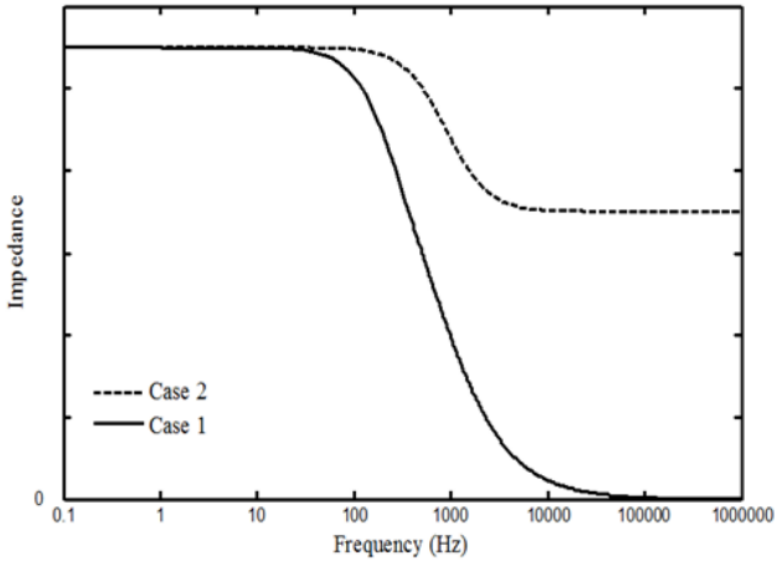

Figure 3-7 Impedance curve of Case 1 and Case 2 materials

The shape of the curve of the impedance plot tells us if the material is Case 1 or Case 2. In this study, it was found that all the materials conformed to case 2.

To investigate the effect of corrosion, the electrical impedance response of the corrosion specimens was studied for a set period of days. The cement-steel casing in saltwater was studied for 250 days while the steel bar in moist sand and clay was studied for 70 days. To characterize the electrical response, the impedance curve with frequency was plotted for all the specimens. A method to quantify the surface corrosion was quantified by measuring the contact resistance and contact capacitance. The resistance (R) and capacitance (C) for the bulk material between two points are defined as

$$R = \rho \frac{L}{A} = \rho K \qquad (3-4)$$

$$\text{and } C = \epsilon \frac{A}{L} \qquad (3-5)$$

where A = cross-sectional area, L = distance between the two probes, ρ = resistivity of the material, ϵ = absolute permittivity of the material. The product of equations given in (4) and (5) results as

$$RC = \rho\epsilon. \qquad (3-6)$$

Since ρ and ϵ in equations (3 – 4) and (3 – 5) are material properties, hence RC at the point of contact is also a material property. RC is termed the electrical corrosion index (Vipulanandan et al, 2018) and is used to characterize surface corrosion. The advantage of using this index is that we now can characterize the material property of the corrosion products at the interface level without dependence on the geometry factor such as the length or thickness and area.

CHAPTER 4 EFFECT OF MOISTURE CONTENT ON THE ELECTRICAL RESISTIVITY OF SOIL

4.1 Introduction

In this chapter, the effect of moisture content on the electrical resistivity of two soil types: Ottawa sand and bentonite clay have been studied. A total of eight specimens, four for each type of soil, were prepared with varying moisture contents. In the case of sand the different moisture contents used were: 5%, 10%, 15%, and 20% while in the case of bentonite clay they were: 10%, 20%, 30%, and 40%. For each increment in the moisture content of the specimens, a soil conductivity meter was used to measure the conductivity of the specimen. To get the resistivity value, the reciprocal of the conductivity value was taken. The resistivity data were then plotted against its corresponding moisture content. Two models were used to then predict the data: (1) hyperbolic model and (2) exponential model.

4.2 Results and Discussion

Figure 4-1 depicts the impedance versus frequency plot for the vertical probe configuration of sand and clay specimens with varying moisture contents. From the figure, two observations can be made. First, that as the water content is increased there is a decrease in the impedance value. Second, the impedance value decreases with increasing frequency until up to a certain frequency where it levels off. In this case, at 50 kHz the impedance value begins to level off. This corresponds to case 2: Special bulk material – resistance only (Vipulanandan et al, 2013). This indicates that the impedance of the sand is mostly influenced by the resistance of the material.

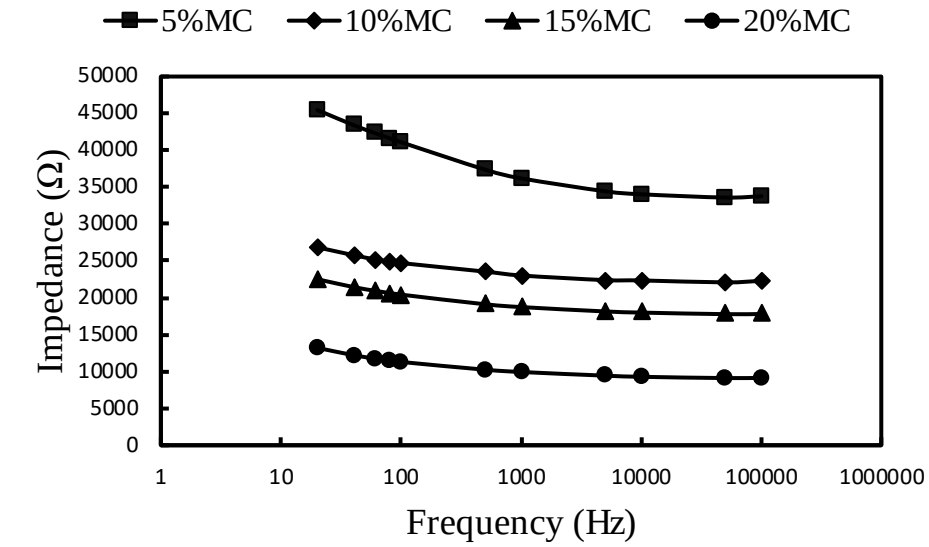

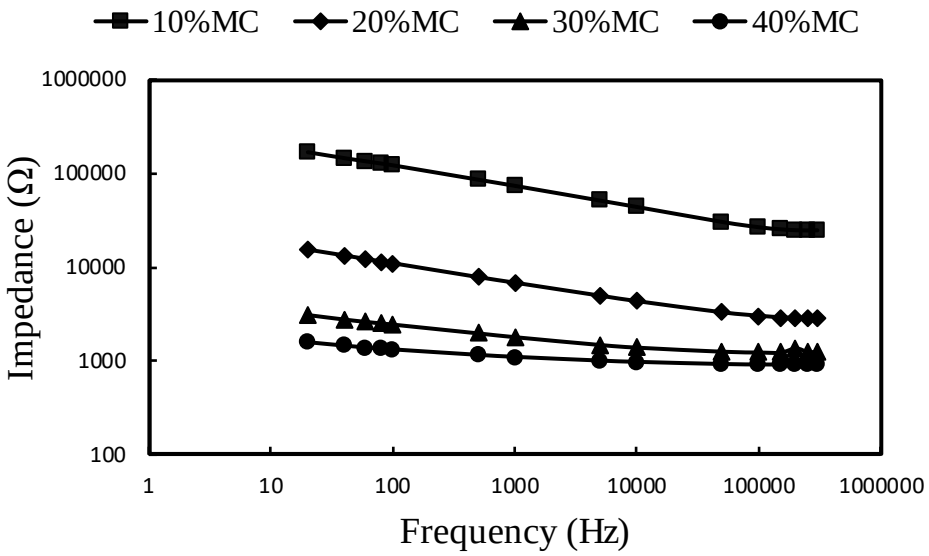

Figure 4-1 Impedance vs frequency plot for the vertical probe configuration with varying moisture content

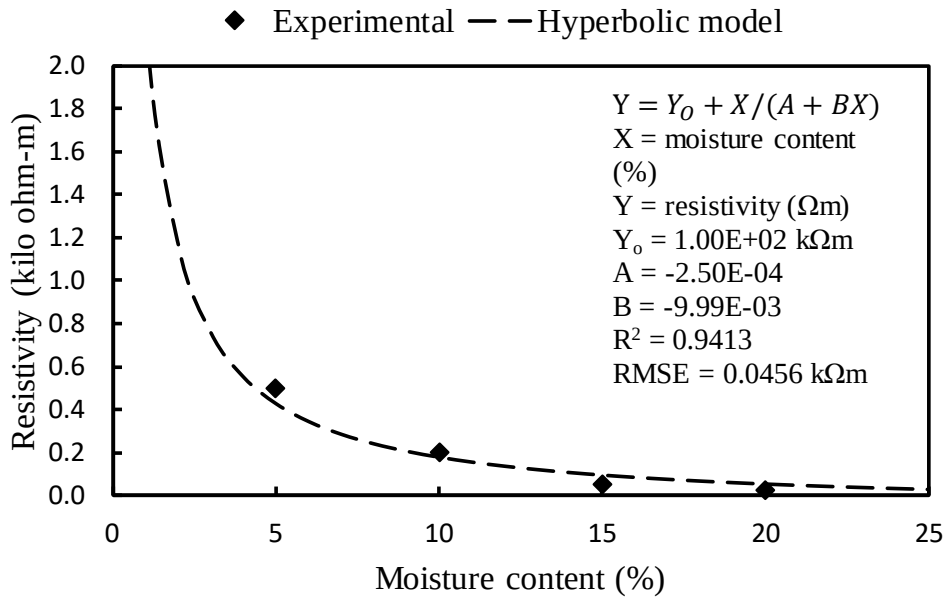

(a)

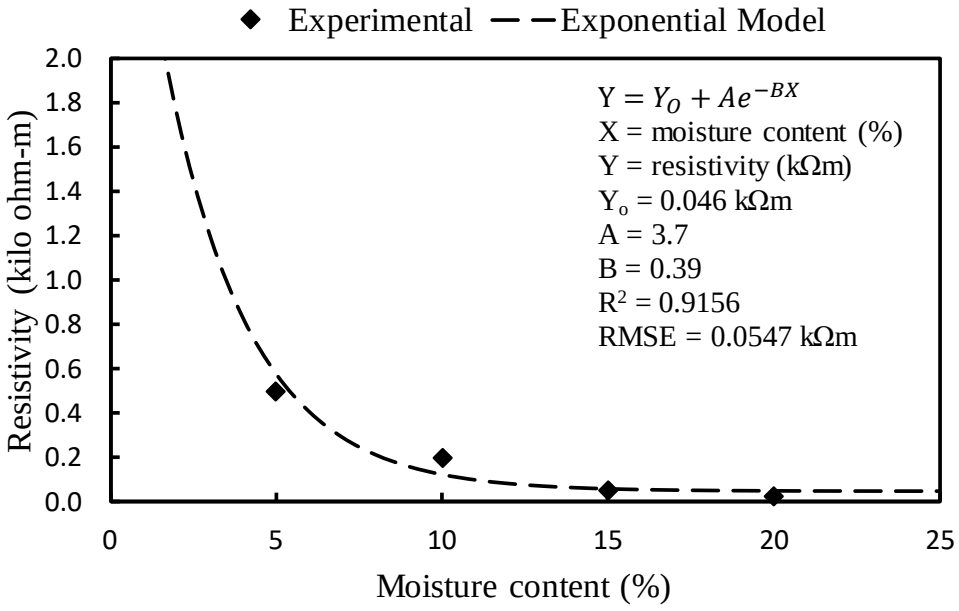

(b)

Figure 4-2 Experimental resistivity values and model resistivity values of moist sand as a function of moisture content using (a) Hyperbolic model and (b) Exponential model

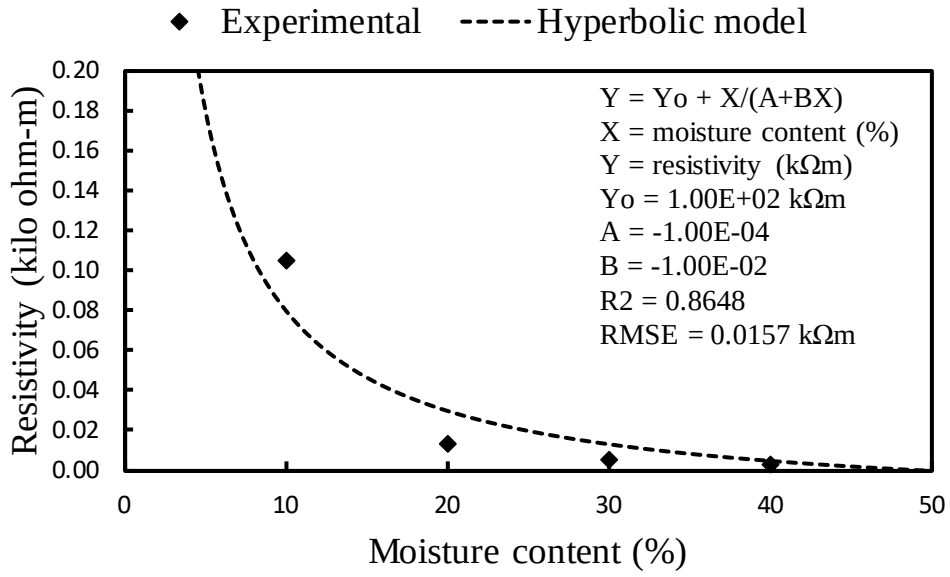

(a)

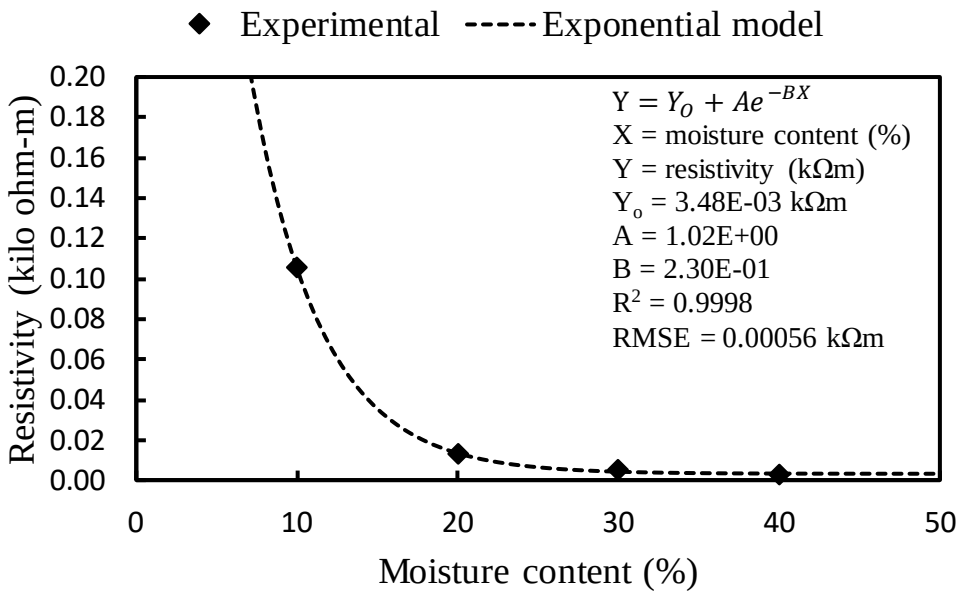

(b)

Figure 4-3 Experimental resistivity values and model resistivity values of moist clay as a function of moisture content using (a) Hyperbolic model and (b) Exponential model

Figures 4-2 and 4-3 depict the experimental resistivity values and model resistivity values of sand and clay as a function of the moisture content. The experimental results indicate that electrical resistivity is significantly influenced by water content, however, this influence is minor when the water content is above 15%. For the sand specimen under study the electrical resistivities with different moisture contents of 10%, 15%, and 20% decrease by 60%, 84.6%, and 94.7%, respectively, when compared with the specimen with the moisture content of 5%. In the case of the clay specimen the electrical resistivities with different moisture contents of 20%, 30%, and 40% decrease by 87.2%, 94.9%, and 97.3%, respectively, when compared with the specimen with the moisture content of 10%. This phenomenon corresponds to the onset of saturation conditions in the sand for which the resistivity value remains nearly constant.

This observation can be explained by the fact that dry sand has a very high value of electrical resistivity (Fukue et al, 1999). The resistivity of sandy soil primarily depends on the amount of permeating fluid, the porosity, and the pore continuity of the sandy soil (Zhou et al, 2015). Hence, for a slight increase in the water content, we can see a significant amount of decrease in the resistivity value. The same phenomenon can also be observed in the clay specimen as well.

Two functions were used to model the experimental resistivity data points: (1) the hyperbolic function which takes the form $Y = Y_o + X/(A + BX)$ and (2) the exponential function which takes the form $Y = Y_o + Ae^{-BX}$. Here X is the moisture content (%), Y is the resistivity value (kΩm), and A and B are model constants. The two equations provided a good fit for the experimental resistivity values of both the soil specimens. In the case of the sand specimen, the Hyperbolic model gave a root mean square error (RMSE) of 0.0456 kΩm while the Exponential model gave an RMSE value of 0.0547 kΩm. For the clay specimen, the Hyperbolic model and Exponential model returned an RMSE value of 0.0157 kΩm AND 0.00056 kΩm, respectively.

4.3 Summary

From the study of the effect of moisture content on the electrical resistivity of Ottawa sand and bentonite clay the following conclusions were drawn:

(1) The resistivity of Ottawa sand and bentonite clay is dependent on the amount of permeating fluid, the porosity, and the pore continuity of the sand specimen. Thus, the resistivity value drops for higher water content and after saturation, the value remains constant.

(2) The impedance value of Ottawa sand and bentonite clay over the frequency range of 20 Hz to 100 kHz (for the given water content) decreases from 20 Hz to 50 kHz beyond which it becomes nearly constant. This behavior shown by the two soil signifies that the impedance of both sand and clay is mostly influenced by the bulk resistance. Hence, it follows case 2.

(3) In the case of sand, the maximum change in resistance and resistivity occurred in the range of 5 to 15 percent water content while in the case of clay the maximum change occurred in the range of 10% to 20% moisture content. After that, the change was rather minuscule.

(4) The Hyperbolic function and Exponential function were successfully used to model the resistivity data for the varying moisture contents.

CHAPTER 5 CORROSION STUDY OF STEEL CASING IN CEMENT-STEEL CASING IMMERSED IN 3.5 PERCENT SALINE SOLUTION

5.1 Introduction

In this chapter, the corrosion of cement-steel casing in 3.5% NaCl solution has been investigated over 250 days. The change in the resistance, contact resistance, contact capacitance, interface resistance, and interface capacitance has been quantified using the Vipulanandan Impedance Model.

5.2 Corrosion Quantification of Cement-steel casing in Saline Environment

The impedance-frequency measurements of the cement-steel casing immersed in 3.5% NaCl solution were monitored for 250 days. The impedance was measured using a commercial LCR device over a frequency range of 20 Hz to 300 kHz. The electrical impedance data was then collected and plotted as a function of the frequency. It was observed that the impedance curve corresponds to case 2 of the Vipulanandan Impedance Model, wherein the bulk material is represented by a resistor and the contacts are represented by a resistor and capacitor in parallel. The bulk resistance, contact resistance, and contact capacitance for the various probe configurations were computed by optimizing the model impedance data points in the MS EXCEL program.

5.2.1 Corrosion in Cement Measured Along Vertical Direction

The impedance versus frequency plot of the vertical configuration (C3-C4) of the cement is shown in Figure 5-1. The model parameters obtained from optimization of the impedance model are summarized in Table 5-1. After immersion, the bulk resistance was 1087 Ω and it increased to 1126 Ω, 1941 Ω, 2370 Ω, and 2486 Ω after 10 days, 50 days, 100 days, and 250 days of immersion in a 3.5 % NaCl solution. The contact resistance of contact #3 increased from an initial value of 676 Ω to 798 Ω, 792 Ω, 841 Ω and 1118 Ω after 10 days, 50 days, 100 days, and 250 days, respectively. Similarly, the contact resistance of contact #4 increased from an initial value of 595 Ω to 679 Ω, 944 Ω, 1181 Ω, and 1526 Ω after 10 days, 50 days, 100 days, and 250 days,

respectively. The change in resistance activity shows the ongoing phenomenon of corrosion inside the cement specimen.

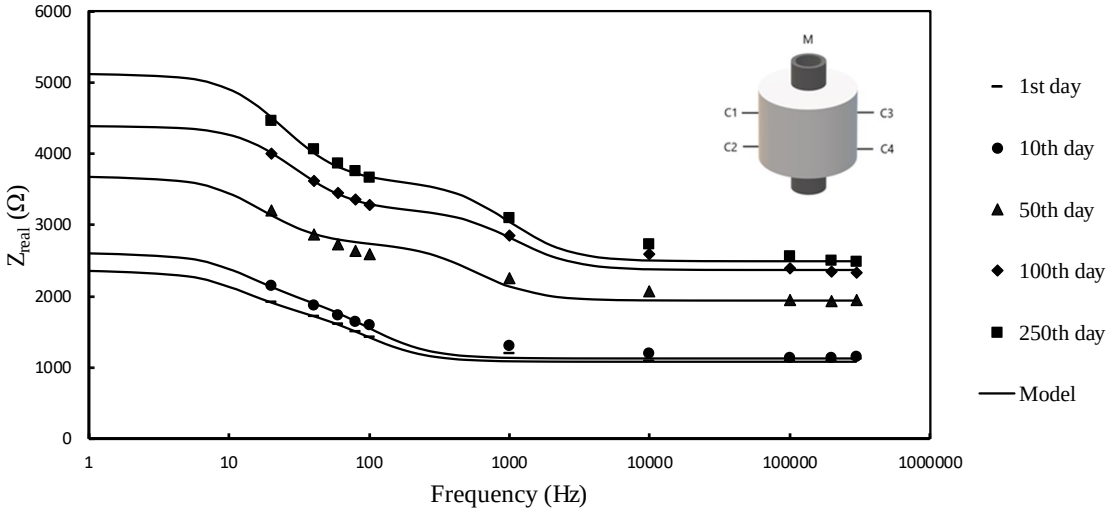

Figure 5-1 Impedance behavior of cement-steel casing in salt solution measured over time for the vertical configuration (C3-C4)

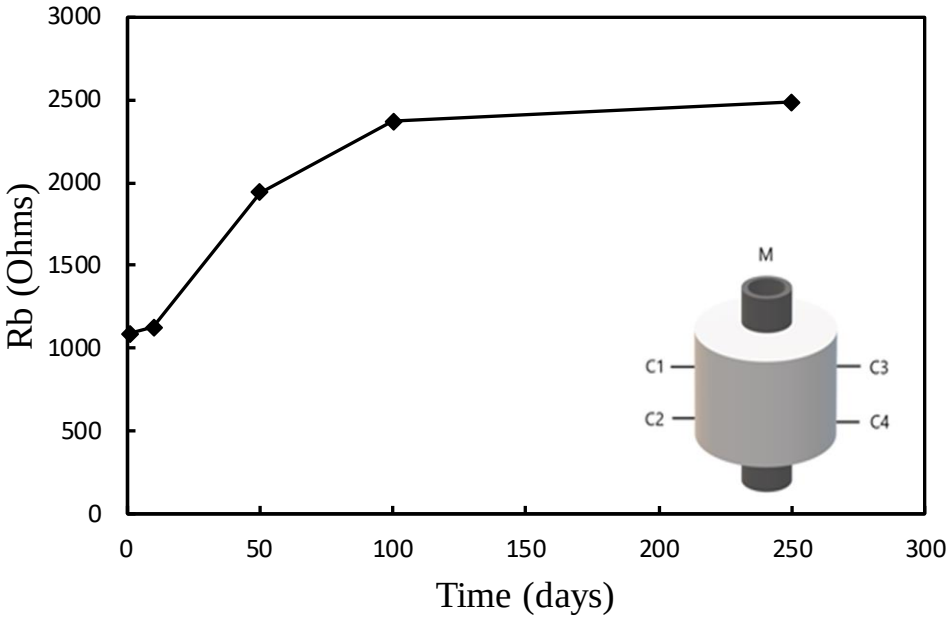
Rb (Ohms)
Time (days)
M
C1
C2
C3
C4

(a)

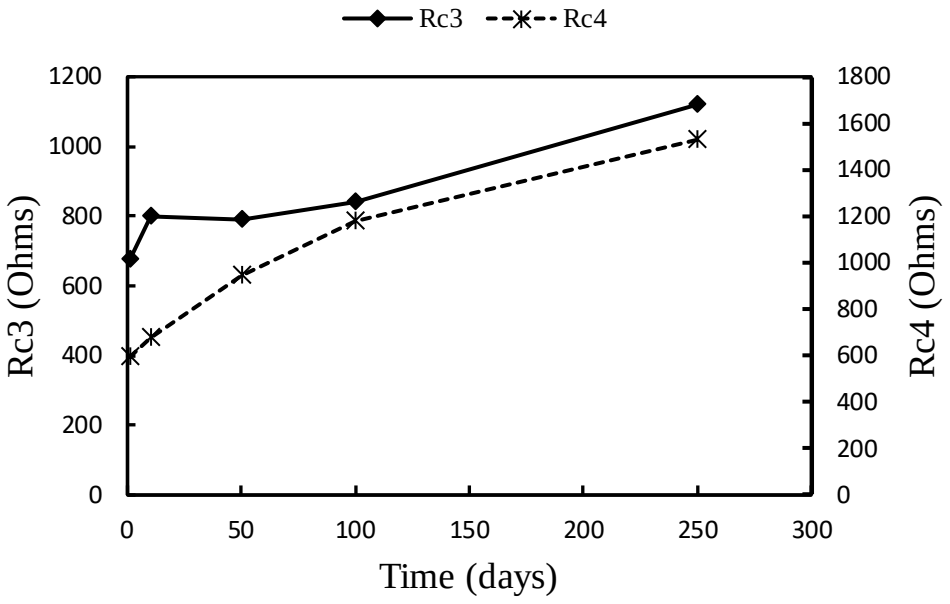
Rc3
Rc4
Rc3 (Ohms)
Rc4 (Ohms)
Time (days)

(b)

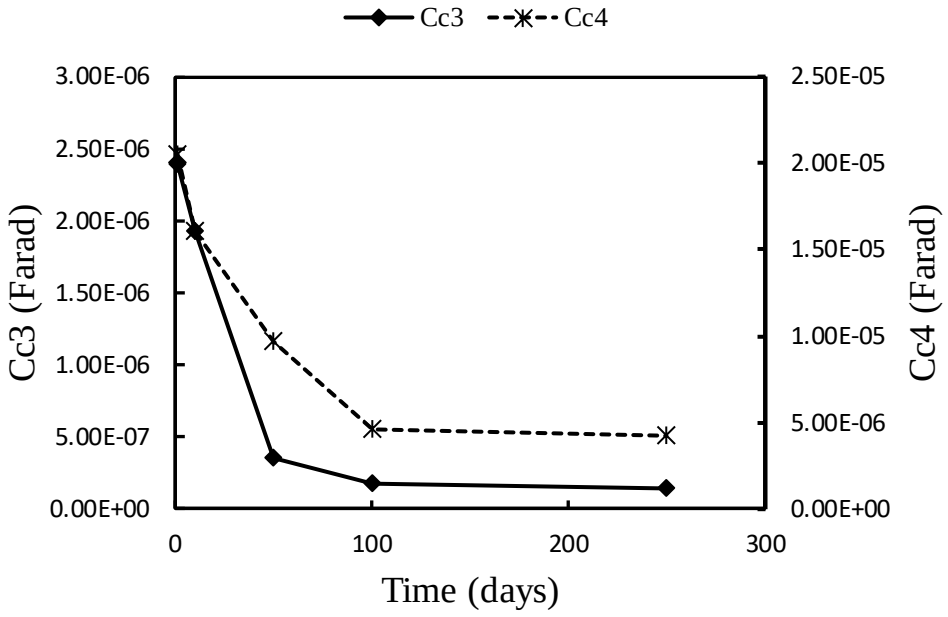

(c)

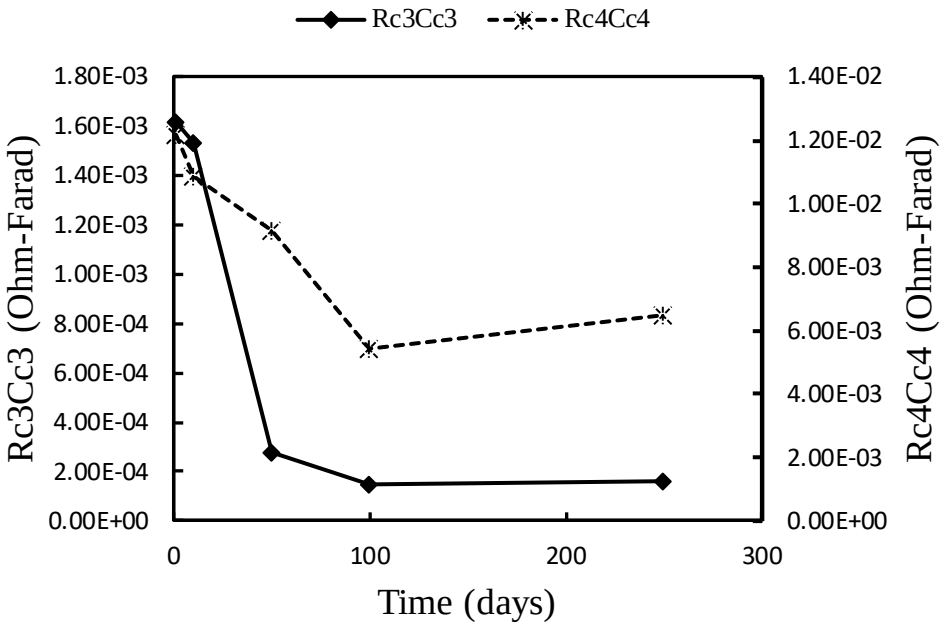

(d)

Figure 5-2 Changes in (a) bulk resistance (Rb), (b) contact resistance (Rc), (c) contact capacitance (Cc), and (d) corrosion index (RcCc) of cement-steel casing in salt solution over time for the vertical configuration (C3-C4)

Table 5-1 Model parameters of the equivalent circuit for the vertical configuration (C3-C4) of the cement-steel casing in salt solution

Days	Rb	Rc3	Cc3	Rc4	Cc4	Rc3Cc3	Rc4Cc4	R^2	RMSE
1	1086.65	676.00	2.40E-06	595.00	2.05E-05	1.62E-03	1.22E-02	0.9864	33.62
10	1126.31	798.00	1.92E-06	678.50	1.60E-05	1.54E-03	1.09E-02	0.9687	60.60
50	1941.21	792.00	3.48E-07	944.50	9.71E-06	2.76E-04	9.17E-03	0.9513	87.36
100	2370.27	841.00	1.73E-07	1181.00	4.59E-06	1.46E-04	5.42E-03	0.9552	112.53
250	2486.45	1118.00	1.43E-07	1525.50	4.25E-06	1.60E-04	6.48E-03	0.9660	119.23

The contact capacitance of contact #3, on the other hand, decreased from the initial observed value of 2.40e-06 F to 1.92e-06 F, 3.48e-07 F, 1.73e-07 F, and 1.43e-07 F after 10 days, 50 days, 100 days, and 250 days, respectively. Similarly, the contact capacitance of contact #4 decreased from the initial observed value of 2.05e-05 F to 1.60e-05 F, 9.71e-06 F, 4.59e-06 F, and 4.25e-06 F after 10 days, 50 days, 100 days and 250 days, respectively. The coefficient of determination and root mean square error observed after the immersion interval of 10 days, 50 days, 100 days, and 250 days were 0.9687, 0.9521, 0.9676, 0.9660 and 60.6 Ω, 86.57 Ω, 95.69 Ω, 119.23 Ω, respectively. Over time the chloride ions get adsorbed onto the C-S-H surface; this adsorption causes the cement resistivity to increase over time. Continuous immersion of cement specimens inside saltwater affects the cement microstructure (Lia et al., 2015 and Yoshida et al., 2002) and leads to the formation of products that affect the cement strength and increases cement resistivity.

The corrosion index RcCc for contact #3 of the vertical combination (C3-C4) of the cement decreased by 5.21%, 82.99%, 91%, and 90.15% over 10 days, 50 days, 100 days, and 250 days, respectively while for contact #4 it decreased by 10.57%, 24.7%, 55.49% and 46.76% over 10 days, 50 days, 100 days and 250 days, respectively. The decrease in RcCc can be attributed to the sharp decrease in the value of contact capacitance over the entire immersion period. The contact capacitance at contact #3 decreased by 19.7%, 85.48%, 92.76%, and 94.04% over 10 days, 50 days, 100 days, and 250 days, respectively while at contact #4 it decreased by 21.57%, 52.56%, 77.58% and 79.23% over 10 days, 50 days, 100 days and 250 days, respectively.

5.2.2 Corrosion at the Interface of Steel Casing and Cement-steel casing

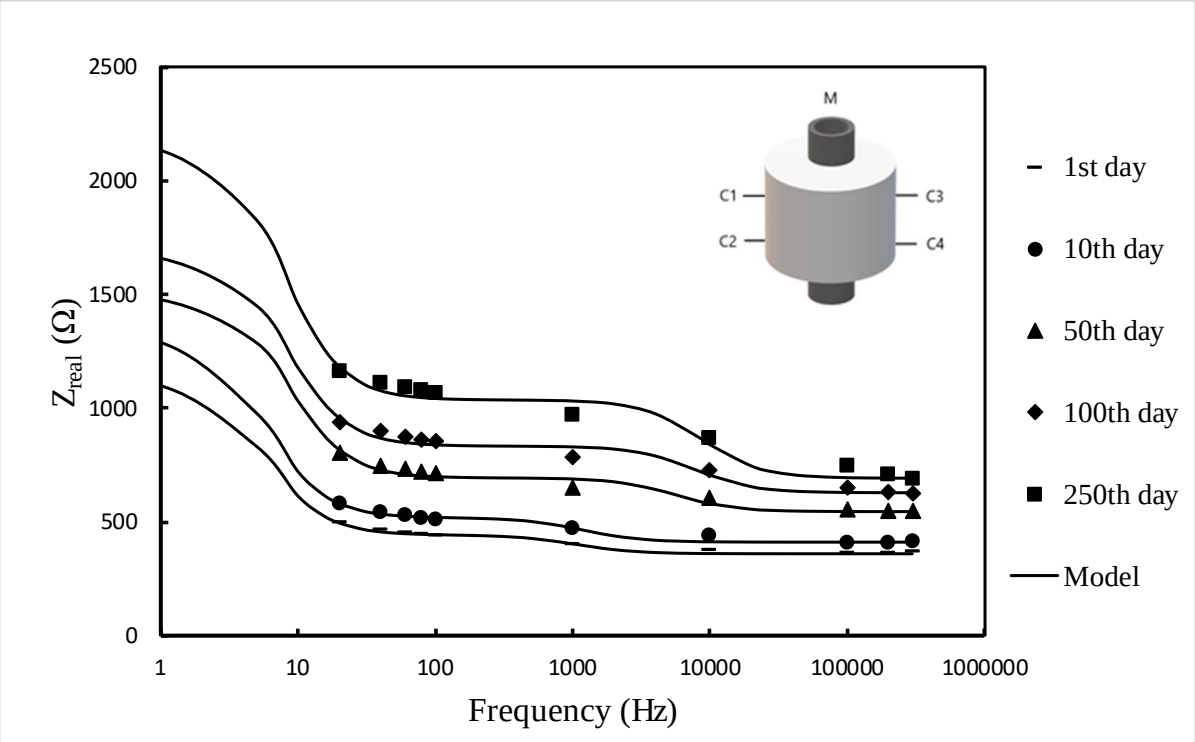

Figure 5-3 Impedance behavior of cement-steel casing in salt solution measured over time for M-C3 configuration

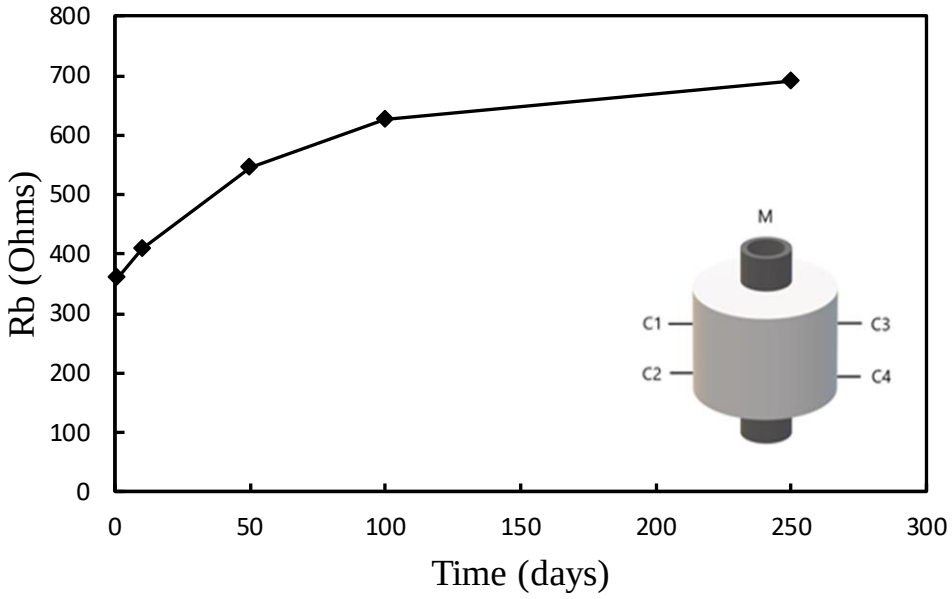
800
700
600
500
400
300
200
100
0
Rb (Ohms)
0
50
100
150
200
250
300
Time (days)
M
C1
C2
C3
C4

(a)

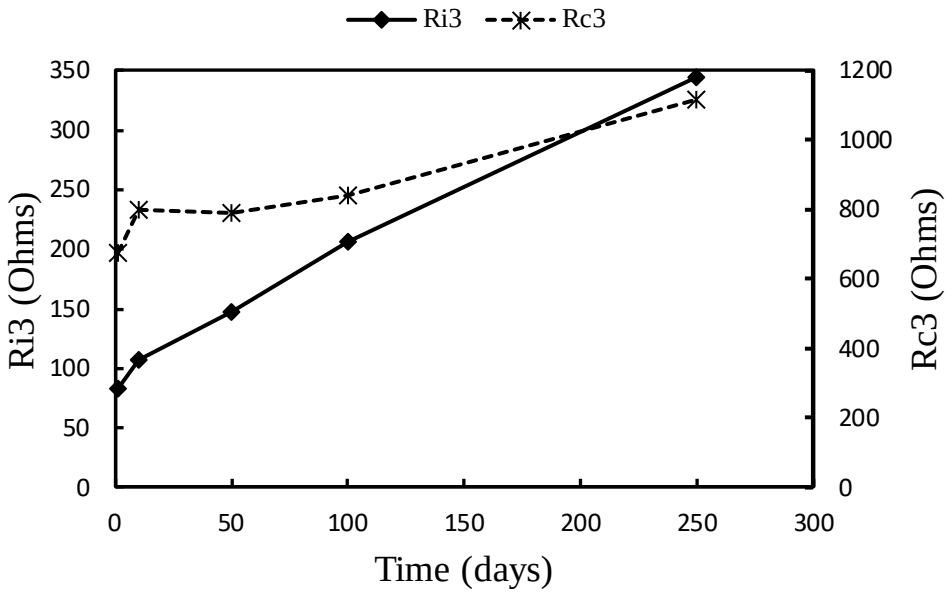
Ri3
Rc3
350
300
250
200
150
100
50
0
Ri3 (Ohms)
1200
1000
800
600
400
200
0
Rc3 (Ohms)
0
50
100
150
200
250
300
Time (days)

(b)

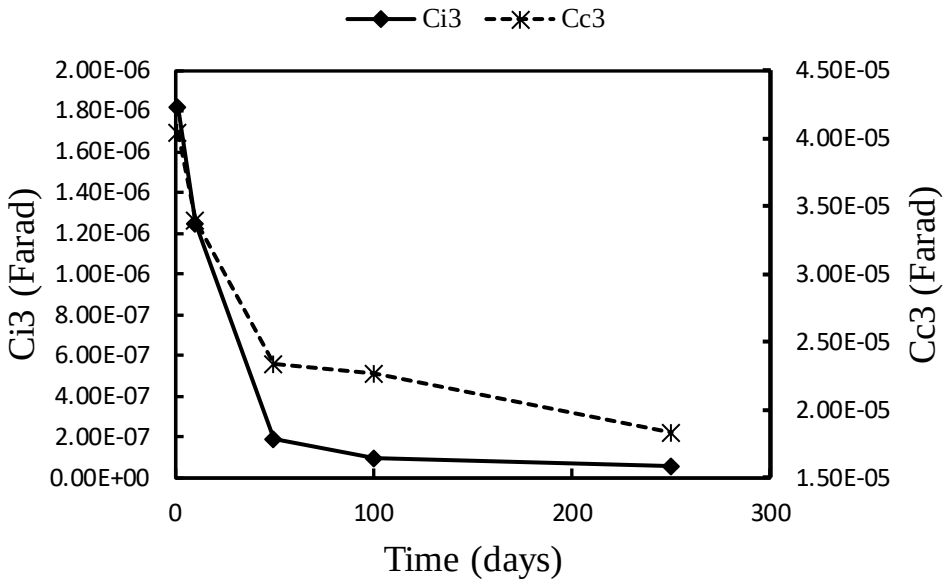

(c)

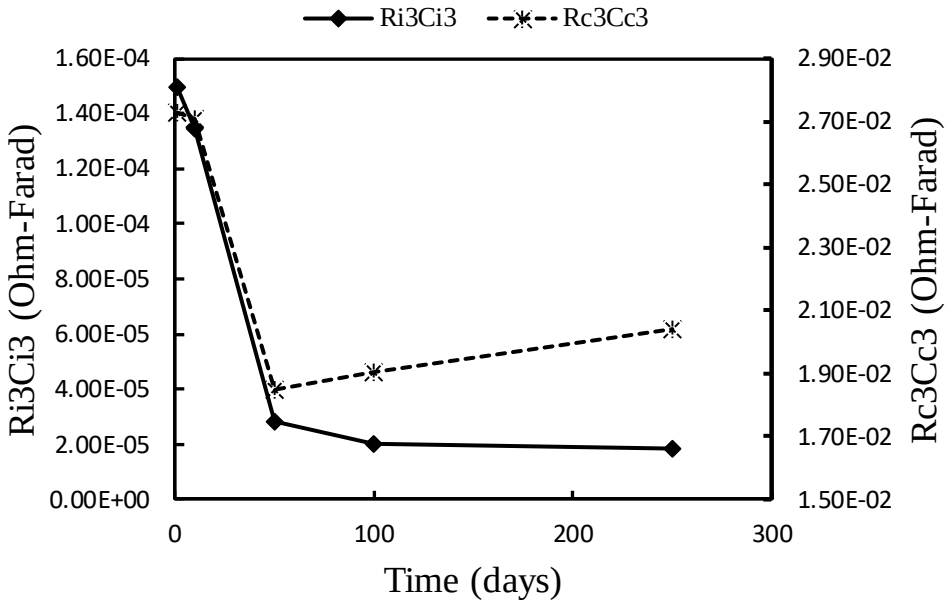

(d)

Figure 5-4 Changes in (a) bulk resistance (Rb), (b) contact resistance (Rc), (c) contact capacitance (Cc), and (d) corrosion index (RcCc) of cement-steel casing in salt solution over time for M-C3 configuration

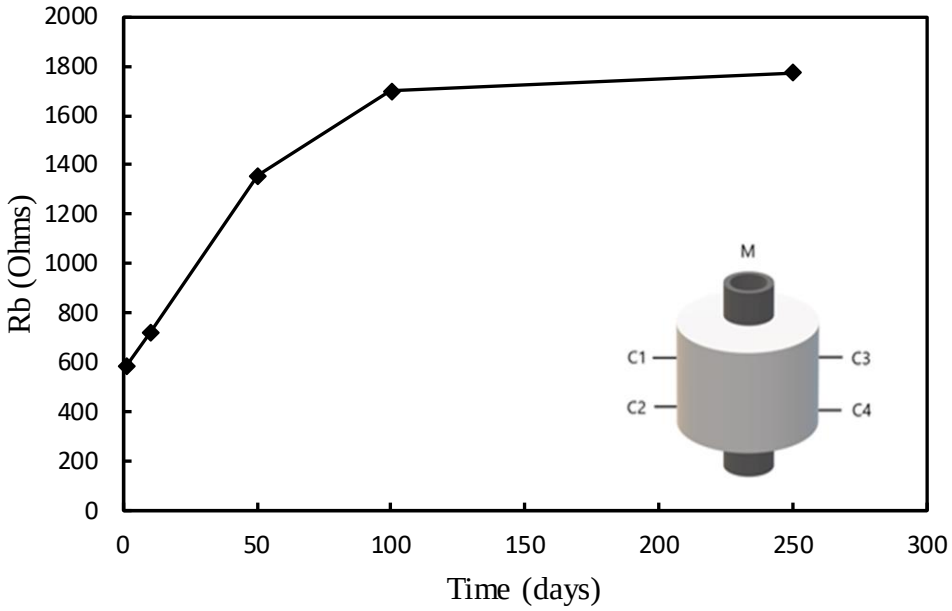
Rb (Ohms)
Time (days)
M
C1
C2
C3
C4

(a)

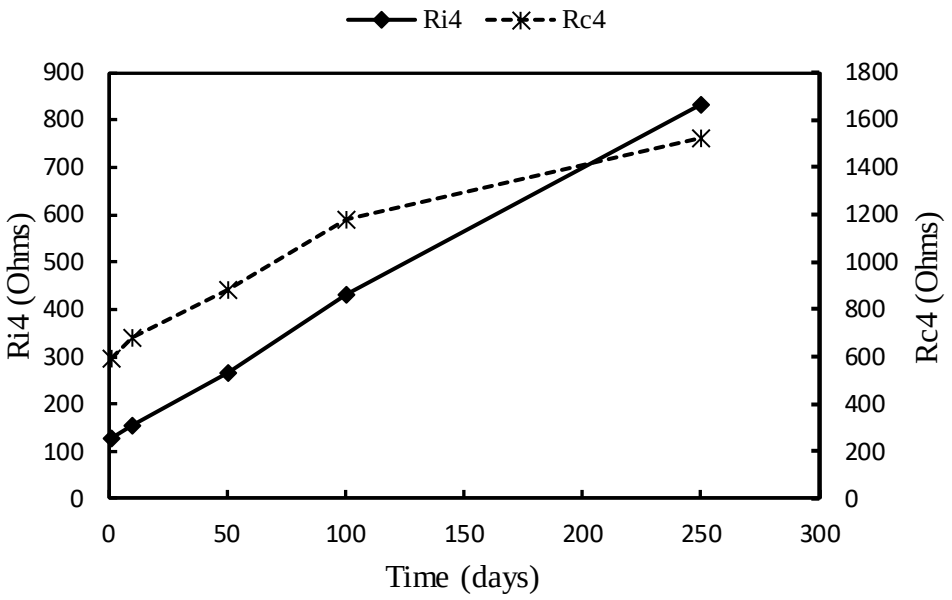
Ri4
Rc4
Ri4 (Ohms)
Rc4 (Ohms)
Time (days)

(b)

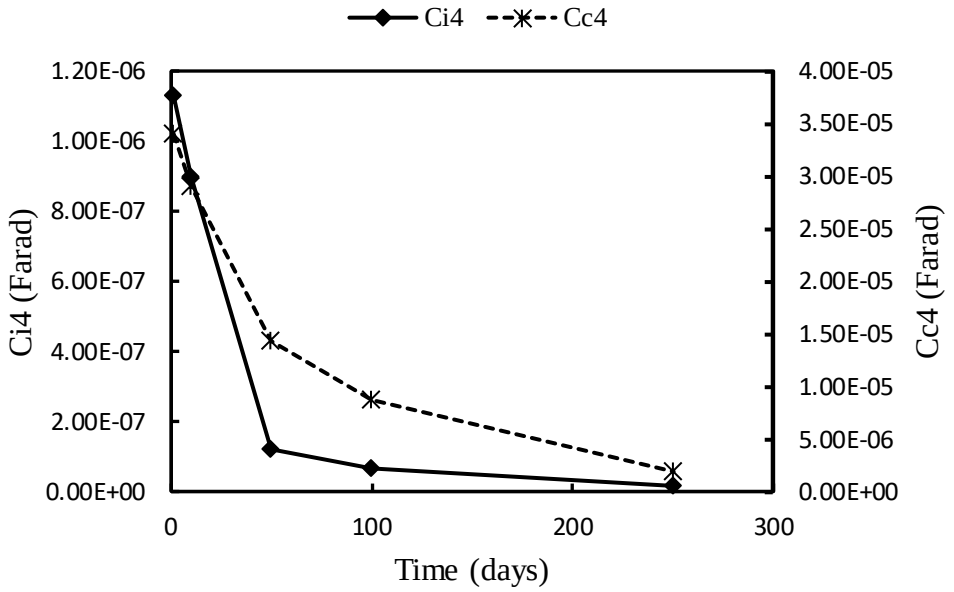

(c)

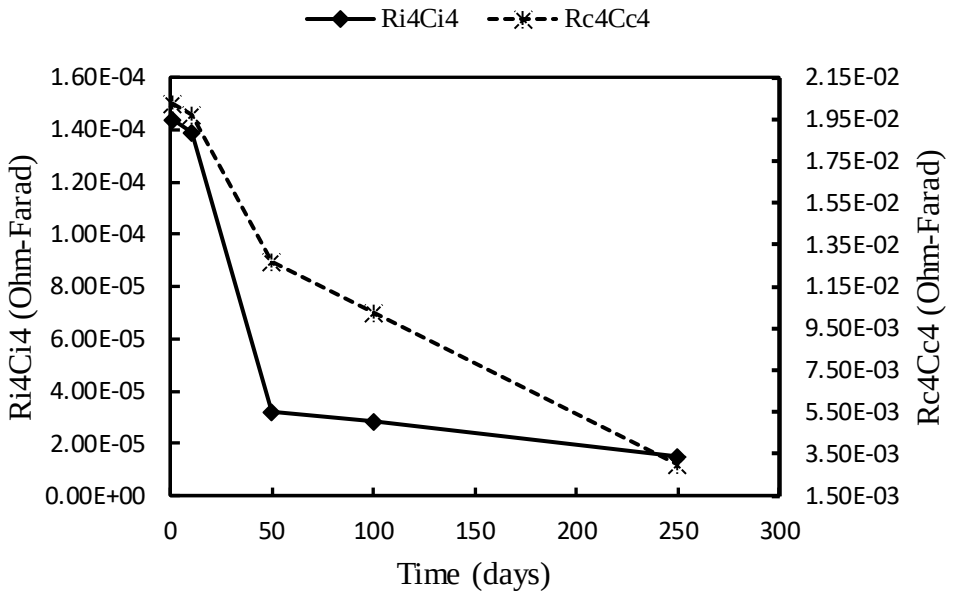

(d)

Figure 5-5 Changes in (a) bulk resistance (Rb), (b) contact resistance (Rc), (c) contact capacitance (Cc), and (d) corrosion index (RcCc) of cement-steel casing in salt solution over time for M-C4 configuration

Table 5-2 Model parameters of the equivalent circuit for M-C3 configuration of the cement-steel casing in salt solution

Days	Rb	Ri3	Ci3	Rc3	Cc3	Ri3Ci3	Rc3Cc3	R^2	RMSE
1	361.58	82.39	1.82E-06	676.00	4.04E-05	1.50E-04	2.73E-02	0.9792	6.55
10	408.94	107.67	1.25E-06	798.00	3.40E-05	1.35E-04	2.71E-02	0.9744	9.34
50	547.02	147.63	1.93E-07	792.00	2.33E-05	2.85E-05	1.85E-02	0.9513	18.91
100	626.74	205.69	9.93E-08	841.00	2.26E-05	2.04E-05	1.90E-02	0.9455	25.13
250	691.08	344.86	5.31E-08	1118.00	1.83E-05	1.83E-05	2.04E-02	0.9424	39.97

Table 5-3 Model parameters of the equivalent circuit for M-C4 configuration of the cement-steel casing in salt solution

Days	Rb	Ri4	Ci4	Rc4	Cc4	Ri4Ci4	Rc4Cc4	R^2	RMSE
1	584.68	127.35	1.13E-06	595.00	3.40E-05	1.44E-04	2.02E-02	0.9792	10.10
10	722.29	155.30	8.96E-07	678.50	2.91E-05	1.39E-04	1.97E-02	0.9785	12.52
50	1357.28	265.72	1.21E-07	885.50	1.43E-05	3.21E-05	1.27E-02	0.9577	32.99
100	1700.65	430.78	6.62E-08	1181.00	8.67E-06	2.85E-05	1.02E-02	0.9551	55.97
250	1772.05	831.43	1.81E-08	1525.50	1.96E-06	1.50E-05	2.99E-03	0.9813	92.25

Table 5-4 Change in model parameters over time for M-C3 configuration of the cement-steel casing in salt solution

Days	Change in Rb	Change in Ri3	Change in Ci3	Change in Rc3	Change in Cc3	Change in Ri3Ci3	Change in Rc3Cc3
10	13.10%	30.67%	-31.13%	18.05%	-15.84%	-10.00%	-0.65%
50	51.29%	79.18%	-89.38%	17.16%	-42.19%	-80.98%	-32.27%
100	73.34%	149.65%	-94.53%	24.41%	-43.92%	-86.35%	-30.24%
250	91.13%	318.56%	-97.08%	65.38%	-54.77%	-87.78%	-25.19%

Table 5-5 Change in model parameters over time for M-C4 configuration of the cement-steel casing in salt solution

Days	Change in Rb	Change in Ri4	Change in Ci4	Change in Rc4	Change in Cc4	Change in Ri4Ci4	Change in Rc4Cc4
10	23.54%	21.94%	-20.74%	14.03%	-14.39%	-3.35%	-2.37%
50	132.14%	108.64%	-89.33%	48.82%	-57.88%	-77.73%	-37.31%
100	190.87%	238.25%	-94.15%	98.49%	-74.49%	-80.20%	-49.37%
250	203.08%	552.85%	-98.40%	156.39%	-94.24%	-89.57%	-85.24%

The impedance versus frequency plot of M-C3 and M-C4 configuration is shown in Figure 5-3. The model parameters obtained from optimization of the impedance model for the two

configurations are summarized in Table 5-2 and 5-3. After immersion, the bulk resistance of the M-C3 configuration went up from 361.58 Ω to 691.08 Ω for 250 days of immersion in a 3.5 % NaCl solution. The bulk resistance for configuration M-C4 went up from 584.68 Ω to 1772.05 Ω over the same period of immersion. During the 250 days of immersion time, the interface resistance for M-C3 configuration increased from an initial value of 82.39 Ω to 344.86 Ω. Similarly, the interface resistance for the M-C4 configuration increased from an initial value of 127.35 Ω to 831.43 Ω. The interface capacitance for M-C3 configuration decreased from 1.82E-06 F to 5.31E-08 F while the interface capacitance for M-C4 configuration decreased from 1.13E-06 F to 1.81E-08 F. The interface corrosion index RiCi for configuration M-C3 decreased from 1.50E-04 ΩF to 1.83E-05 ΩF while that for configuration M-C4 decreased from 1.44E-04 ΩF to 1.50E-05 ΩF.

5.3 Summary

In this study, the corrosion behavior of cement-steel casing in a simulated saline environment was studied and modeled using the Vipulanandan Impedance Model. Based on the experimental results the following conclusions can be drawn:

1. The cement-steel casing was allowed to corrode in a simulated saline environment (3.5 % salt solution) for 250 days. To measure the impedance measurements of the sample, a commercial LCR device was used. The electrical resistance readings obtained for the various wire probe configurations of the cement-steel casing showed that the specimen corresponded to Case 2 of the Vipulanandan Impedance Model.
2. For the vertical configuration of the cement-steel casing, the bulk resistance increased from 1087 Ω to 2486 Ω over the 250 days of immersion time. The contact resistance of contact #3 increased from an initial value of 676 Ω to 1118 Ω while the contact resistance of contact #4 increased from an initial value of 595 Ω to 1526 Ω after 250 days, respectively. The contact capacitance of contact #3 decreased from 2.40e-06 F to 1.43e-07 F while the

contact capacitance of contact #4 decreased from 2.05e-05 F to 4.25e-06 F after 250 days, respectively.

3. The interface resistance for M-C3 and M-C4 configuration increased from 82.39 Ω to 344.86 Ω and 127.35 Ω to 831.43 Ω. This increase in the interface resistance suggests that corrosion is occurring at the interface of the cement and steel casing.
4. The corrosion index RcCc for the vertical configuration of the cement-steel casing saw a decrease in its value over the immersion period of 250 days. This behavior of RcCc could be a result of the high rate of decrease in the contact capacitance value which decreased by nearly 90% over the entire immersion period.
5. The interface corrosion index RiCi for the various wire probe configurations of the cement-steel casing saw a decrease in its value over the immersion period of 250 days. This behavior of RiCi could be a result of the high rate of decrease in the interface capacitance value which decreased by over 90% (~97% for M-C3 configuration and ~98% for M-C4 configuration) over the entire immersion period.

CHAPTER 6 CORROSION STUDY OF STEEL BAR IN MOIST SOIL

6.1 Introduction

In this chapter, the corrosion of steel bar in moist soil has been investigated over a period of 70 days. The change in the resistance, contact resistance, contact capacitance, interface resistance and interface capacitance has been quantified using the Vipulanandan Impedance Model.

6.2 Corrosion Quantification of Steel Bar in Moist Sand

Corrosion of steel bar in moist sand (10% moisture content by weight) was studied. The impedance was measured using a commercial LCR device over a frequency range of 20 Hz to 300 kHz. The electrical impedance data was then collected and plotted as a function of the frequency. It was observed that the impedance curve corresponds to case 2 of the Vipulanandan Impedance Model, wherein the bulk material is represented by a resistor and the contacts are represented by a resistor and capacitor in parallel. The bulk resistance, contact resistance and contact capacitance for the various probe configurations were computed by optimizing the model impedance data points in MS EXCEL program.

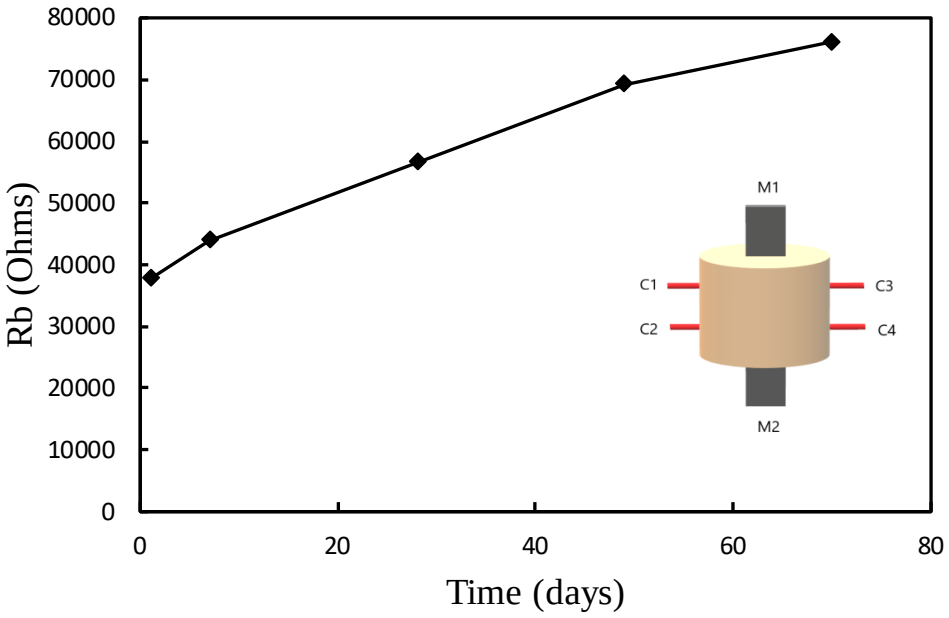
80000
70000
60000
50000
40000
30000
20000
10000
0
Rb (Ohms)
0
20
40
60
80
Time (days)
M1
C1
C3
C2
C4
M2

(a)

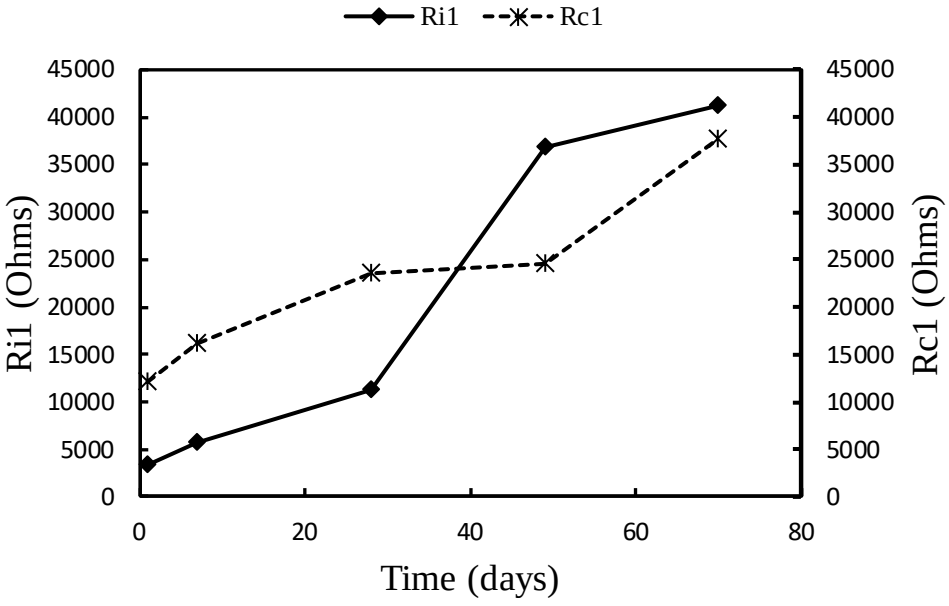
Ri1
Rc1
45000
40000
35000
30000
25000
20000
15000
10000
5000
0
Ri1 (Ohms)
Rc1 (Ohms)
0
20
40
60
80
Time (days)

(b)

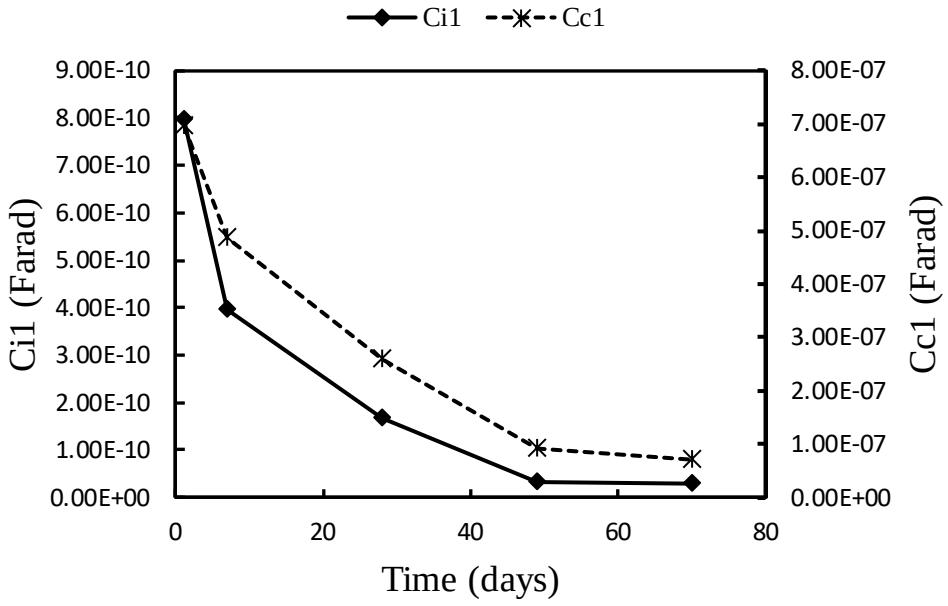

(c)

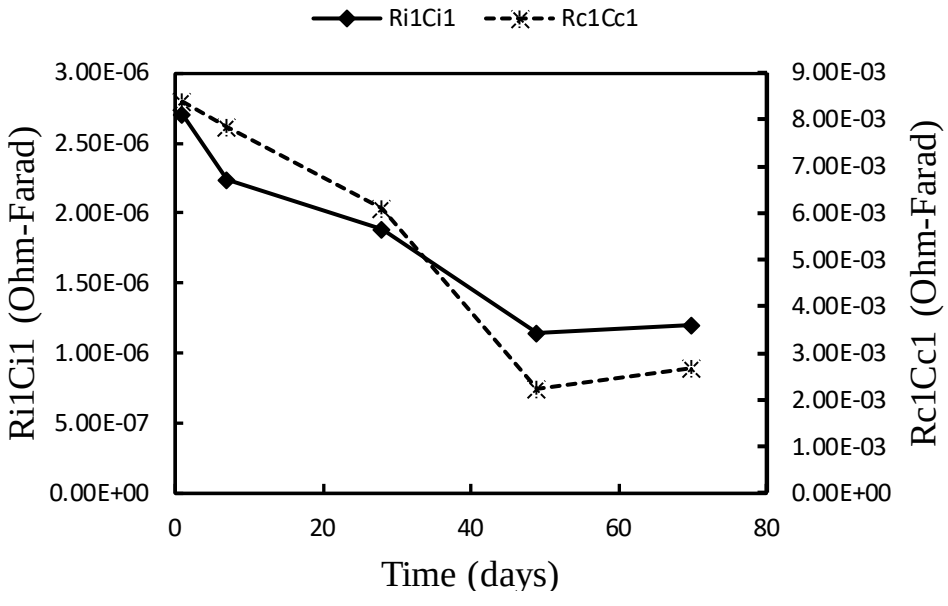

(d)

Figure 6-1 Change in (a) bulk resistance (Rb), (b) interface resistance (Ri) & contact resistance (Rc), (c) interface capacitance (Ci) & contact capacitance (Cc), and (d) corrosion index (RC) over time for M1-C1 configuration of moist sand specimen

Table 6-1 Model parameters of the equivalent circuit for M1-C1 configuration of the moist sand specimen

Days	Rb	Ri1	Ci1	Rc1	Cc1	Ri1Ci1	Rc1Cc1	R^2	RMSE
1	37678.20	3402.63	7.95E-10	12045.78	6.97E-07	2.71E-06	8.40E-03	0.9321	502.80
7	43991.40	5672.92	3.95E-10	16057.50	4.88E-07	2.24E-06	7.83E-03	0.8763	1262.03
28	56625.40	11212.23	1.68E-10	23566.50	2.59E-07	1.89E-06	6.10E-03	0.8821	2039.82
49	69235.90	36776.12	3.12E-11	24611.00	9.11E-08	1.15E-06	2.24E-03	0.9721	2791.92
70	76180.70	41284.83	2.91E-11	37615.50	7.10E-08	1.20E-06	2.67E-03	0.9649	3805.46

Table 6-2 Change in model parameters for M1-C1 configuration of the moist sand specimen

Days	Change in Rb	Change in Ri1	Change in Ci1	Change in Rc1	Change in Cc1	Change in Ri1Ci1	Change in Rc1Cc1
7	16.76%	66.72%	-50.31%	33.30%	-30.01%	-17.15%	-6.70%
28	50.29%	229.52%	-78.85%	95.64%	-62.87%	-30.31%	-27.36%
49	83.76%	980.81%	-96.08%	104.31%	-86.93%	-57.59%	-73.29%
70	102.19%	1113.32%	-96.34%	212.27%	-89.81%	-55.63%	-68.19%

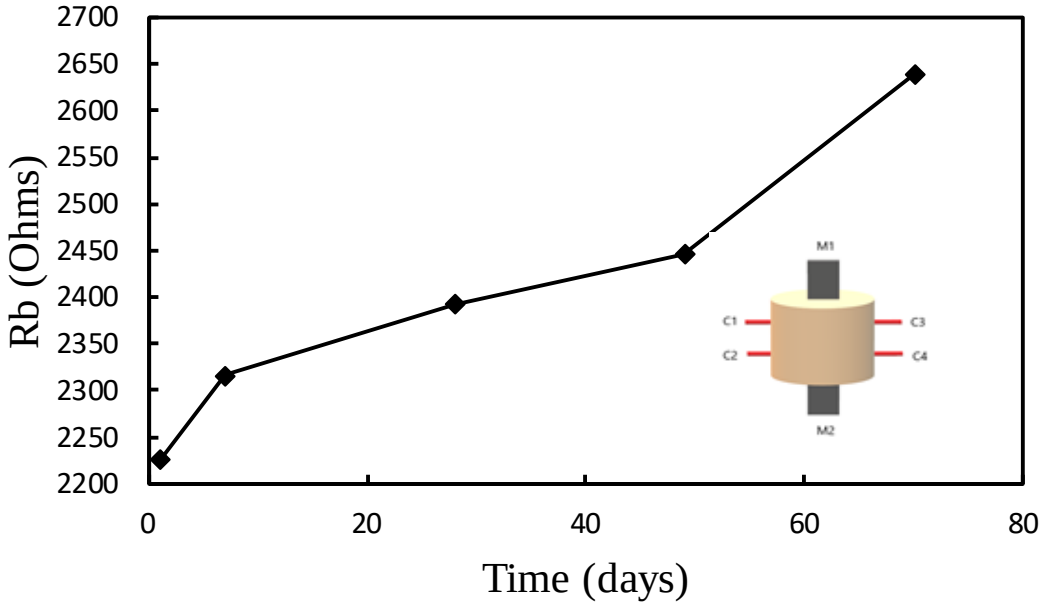
Rb (Ohms)
2700
2650
2600
2550
2500
2450
2400
2350
2300
2250
2200
0
20
40
60
80
Time (days)
M1
C1
C2
C3
C4
M2

(a)

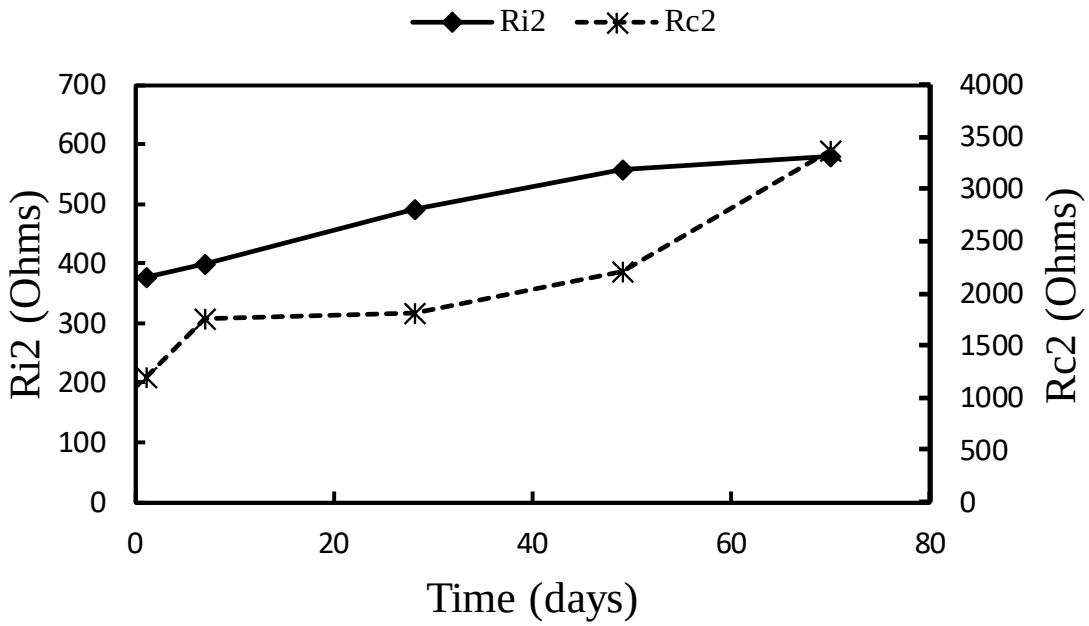
Ri2
Rc2
Ri2 (Ohms)
700
600
500
400
300
200
100
0
Rc2 (Ohms)
4000
3500
3000
2500
2000
1500
1000
500
0
0
20
40
60
80
Time (days)

(b)

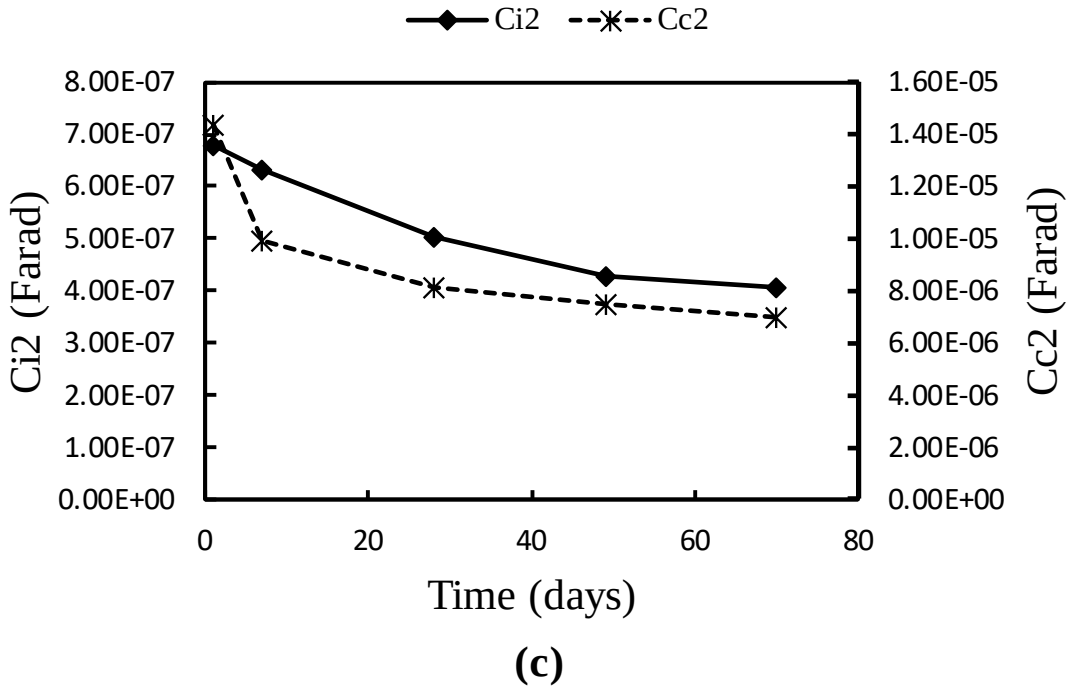

(c)

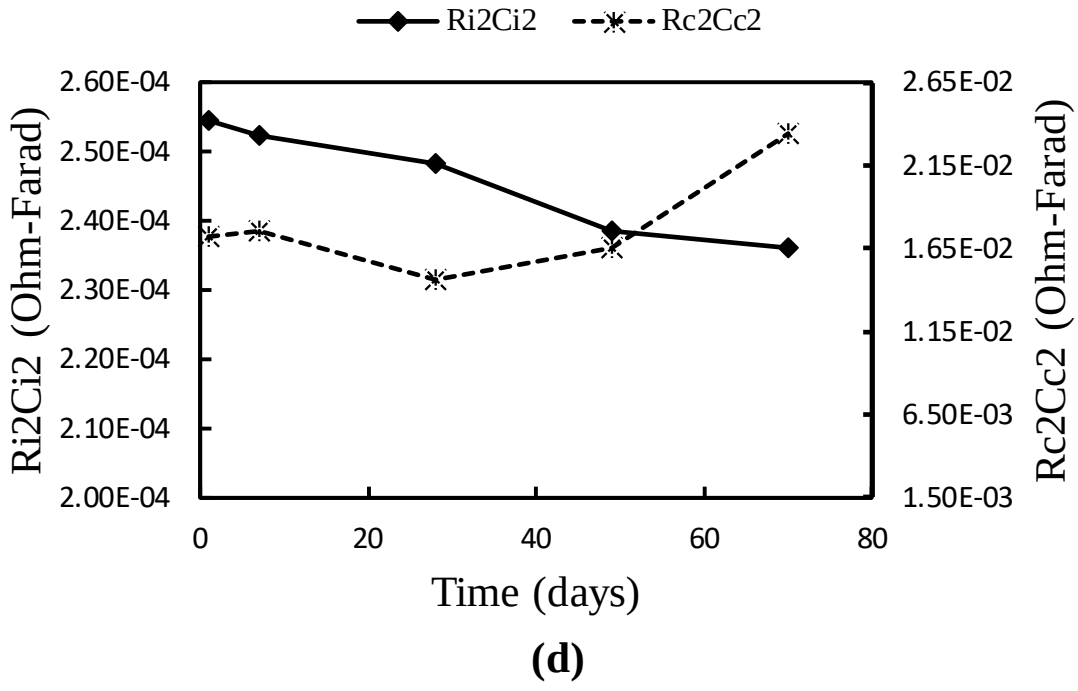

(d)

Figure 6-2 Change in (a) bulk resistance (Rb), (b) interface resistance (Ri) & contact resistance (Rc), (c) interface capacitance (Ci) & contact capacitance (Cc), and (d) corrosion index (RC) over time for M1-C2 configuration of moist sand specimen

Table 6-3 Model parameters of the equivalent circuit for M1-C2 configuration of the moist sand specimen

Days	Rb	Ri2	Ci2	Rc2	Cc2	Ri2Ci2	Rc2Cc2	R^2	RMSE
1	2226.37	375.95	6.77E-07	1198.00	1.43E-05	2.55E-04	1.72E-02	0.9845	28.15
7	2315.92	398.48	6.33E-07	1764.00	9.93E-06	2.52E-04	1.75E-02	0.9628	50.96
28	2393.00	491.85	5.05E-07	1808.50	8.10E-06	2.48E-04	1.46E-02	0.9631	50.26
49	2446.18	557.07	4.28E-07	2214.00	7.47E-06	2.39E-04	1.65E-02	0.9491	59.47
70	2639.11	579.15	4.07E-07	3363.50	6.97E-06	2.36E-04	2.34E-02	0.9571	46.49

Table 6-4 Change in model parameters for M1-C2 configuration of the moist sand specimen

Days	Change in Rb	Change in Ri2	Change in Ci2	Change in Rc2	Change in Cc2	Change in Ri2Ci2	Change in Rc2Cc2
7	4.02%	5.99%	-6.52%	47.25%	-30.70%	-0.92%	2.04%
28	7.48%	30.83%	-25.48%	50.96%	-43.49%	-2.50%	-14.69%
49	9.87%	48.18%	-36.78%	84.81%	-47.86%	-6.32%	-3.63%
70	18.54%	54.05%	-39.84%	180.76%	-51.37%	-7.33%	36.54%

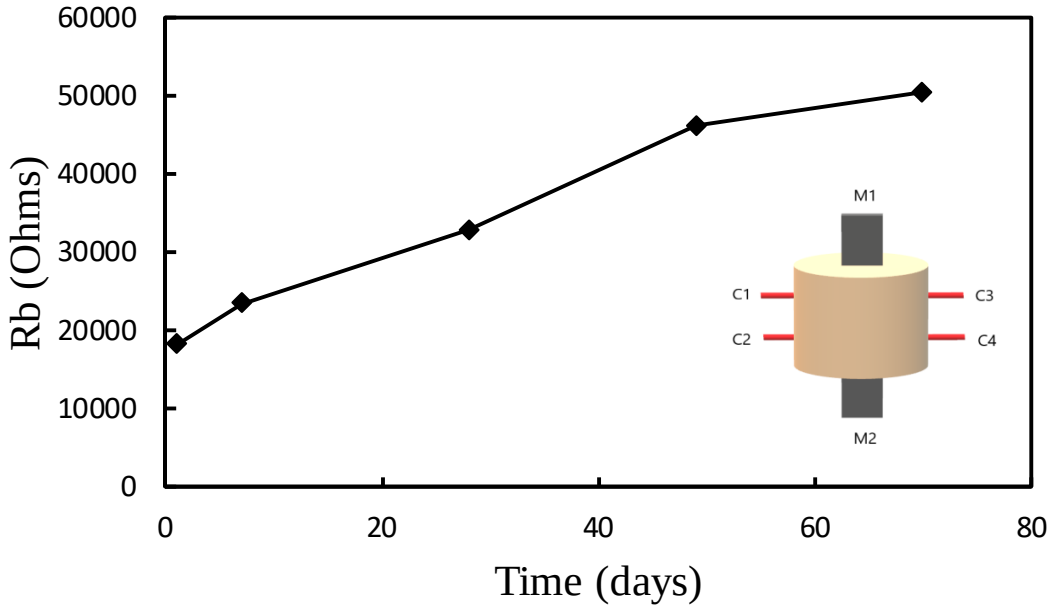
60000
50000
40000
30000
20000
10000
0
Rb (Ohms)
0
20
40
60
80
Time (days)
M1
C1
C2
C3
C4
M2

(a)

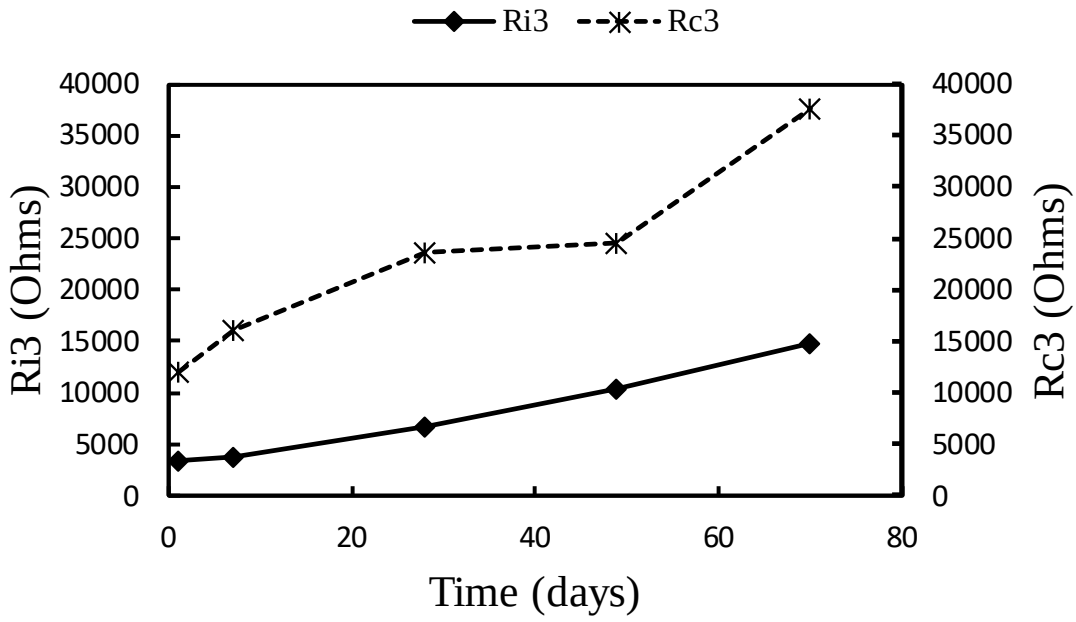
Ri3
Rc3
40000
35000
30000
25000
20000
15000
10000
5000
0
Ri3 (Ohms)
Rc3 (Ohms)
0
20
40
60
80
Time (days)

(b)

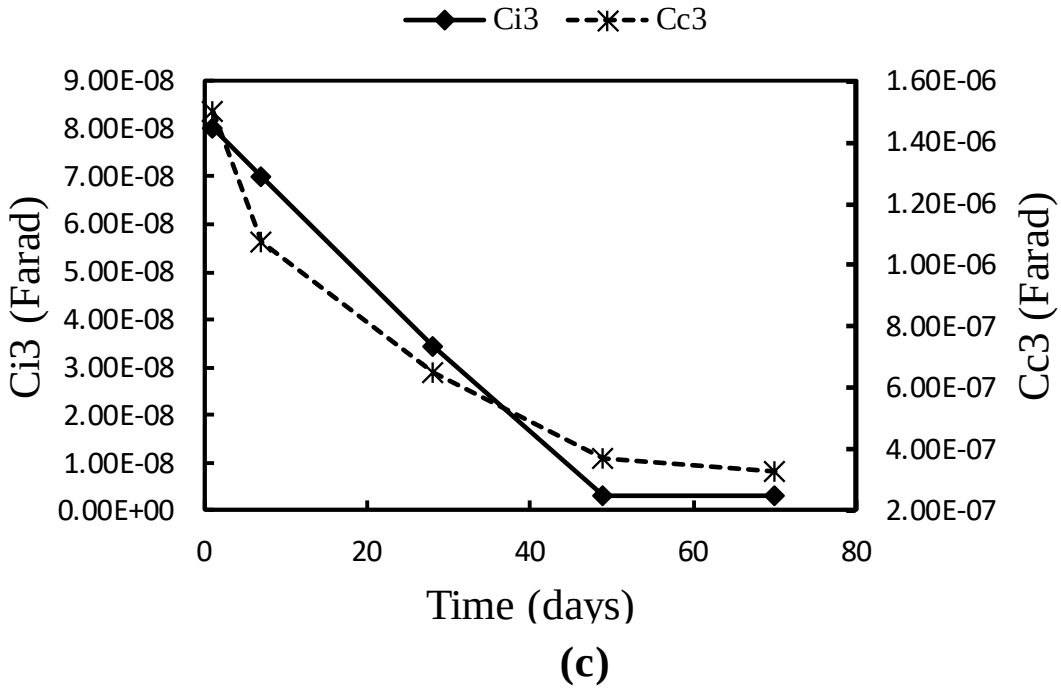

(c)

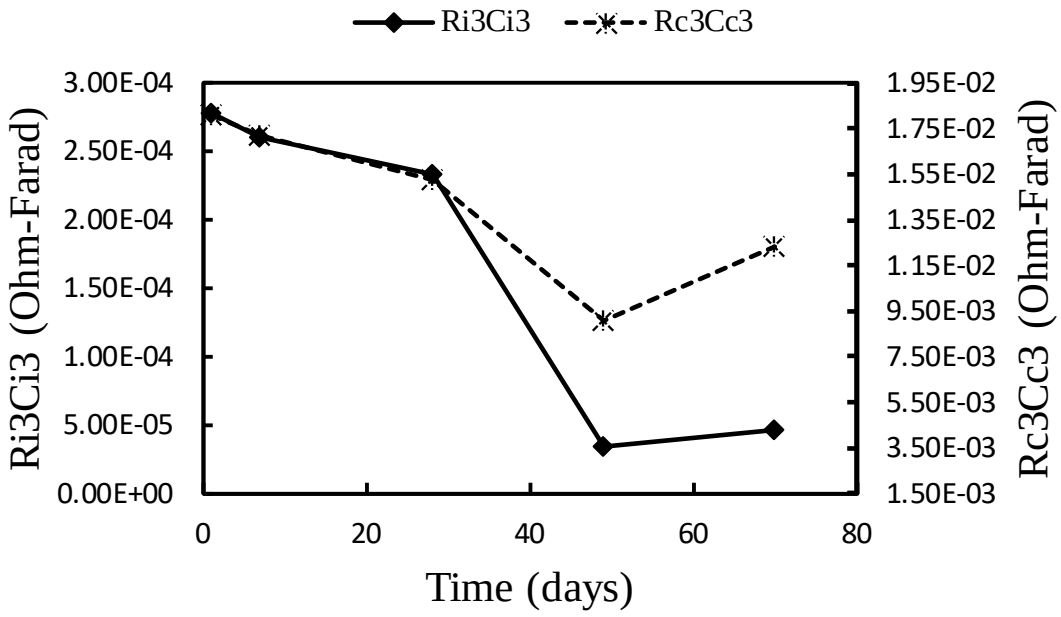

(d)

Figure 6-3 Change in (a) bulk resistance (Rb), (b) interface resistance (Ri) & contact resistance (Rc), (c) interface capacitance (Ci) & contact capacitance (Cc), and (d) corrosion index (RC) over time for M1-C3 configuration of moist sand specimen

Table 6-5 Model parameters of the equivalent circuit for M1-C3 configuration of the moist sand specimen

Days	Rb	Ri3	Ci3	Rc3	Cc3	Ri3Ci3	Rc3Cc3	R^2	RMSE
1	18204.50	3467.50	8.02E-08	12045.78	1.50E-06	2.78E-04	1.81E-02	0.9730	279.62
7	23405.00	3726.90	6.98E-08	16057.50	1.07E-06	2.60E-04	1.72E-02	0.9728	336.69
28	32851.70	6794.77	3.43E-08	23566.50	6.48E-07	2.33E-04	1.53E-02	0.9677	632.99
49	46152.70	10432.90	3.25E-09	24611.00	3.68E-07	3.39E-05	9.07E-03	0.9117	1840.58
70	50491.93	14769.76	3.12E-09	37615.50	3.29E-07	4.61E-05	1.24E-02	0.8335	2784.45

Table 6-6 Change in model parameters for M1-C3 configuration of the moist sand specimen

Days	Change in Rb	Change in Ri3	Change in Ci3	Change in Rc3	Change in Cc3	Change in Ri3Ci3	Change in Rc3Cc3
7	28.57%	7.48%	-12.91%	33.30%	-28.46%	-6.40%	-4.63%
28	80.46%	95.96%	-57.24%	95.64%	-56.77%	-16.22%	-15.43%
49	153.52%	200.88%	-95.95%	104.31%	-75.44%	-87.81%	-49.83%
70	177.36%	325.95%	-96.11%	212.27%	-78.09%	-83.43%	-31.59%

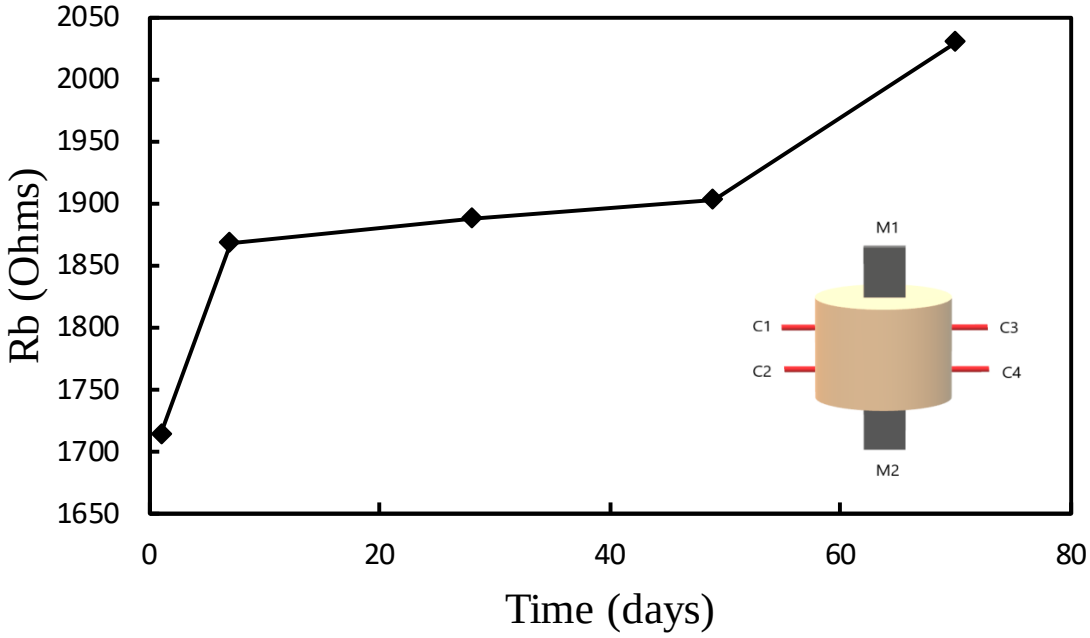
2050
2000
1950
1900
1850
1800
1750
1700
1650
Rb (Ohms)
0
20
40
60
80
Time (days)
M1
C1
C2
C3
C4
M2

(a)

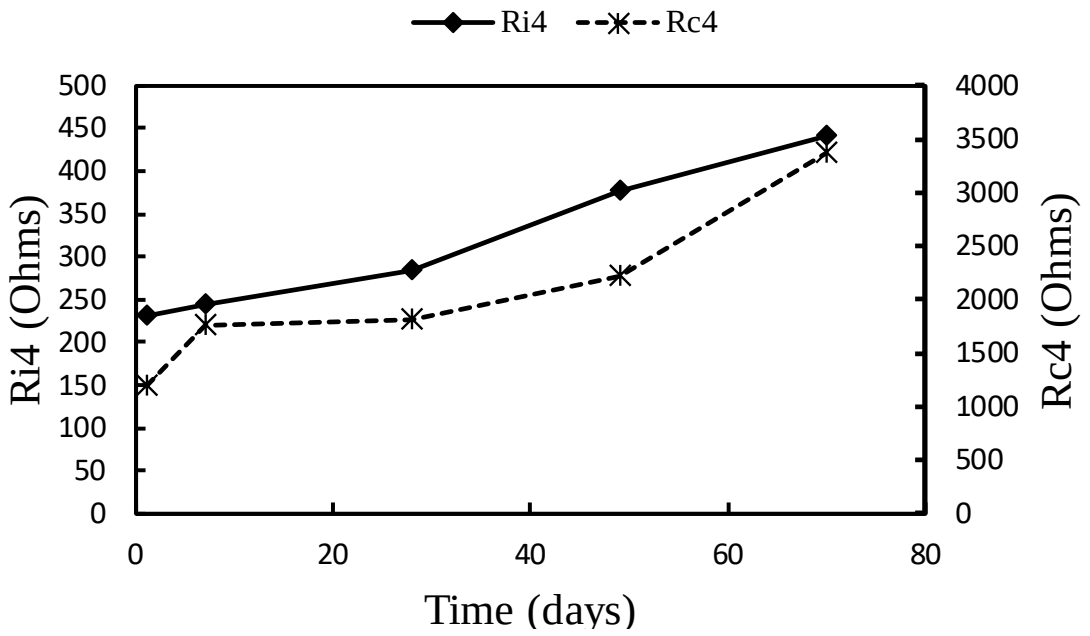
Ri4
Rc4
500
450
400
350
300
250
200
150
100
50
0
Ri4 (Ohms)
4000
3500
3000
2500
2000
1500
1000
500
0
Rc4 (Ohms)
0
20
40
60
80
Time (days)

(b)

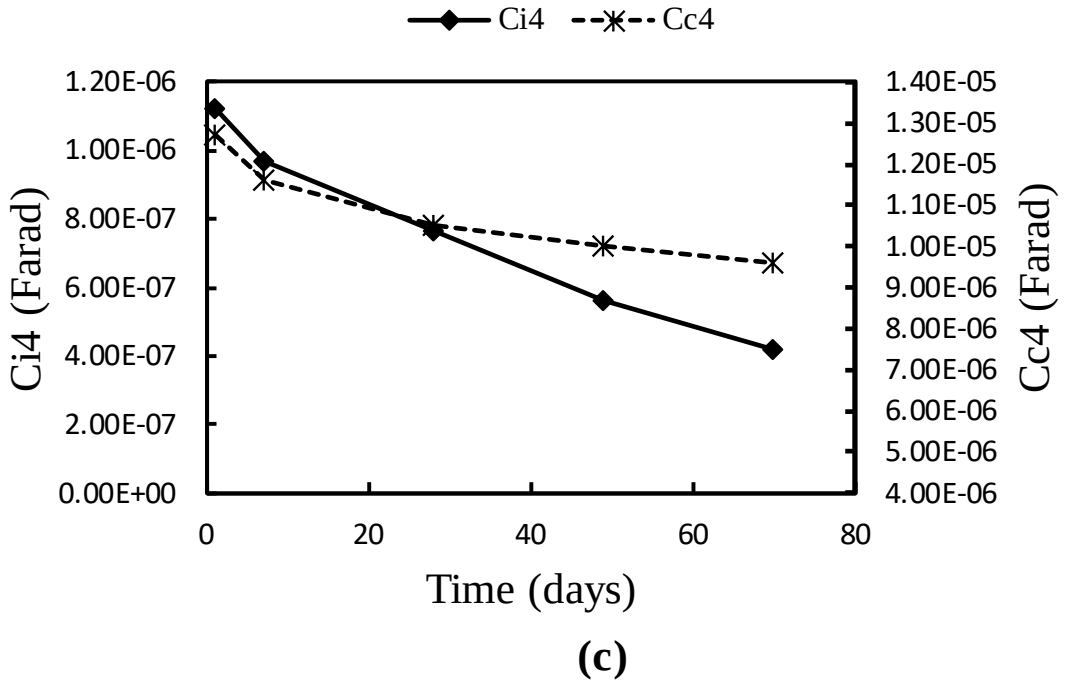

(c)

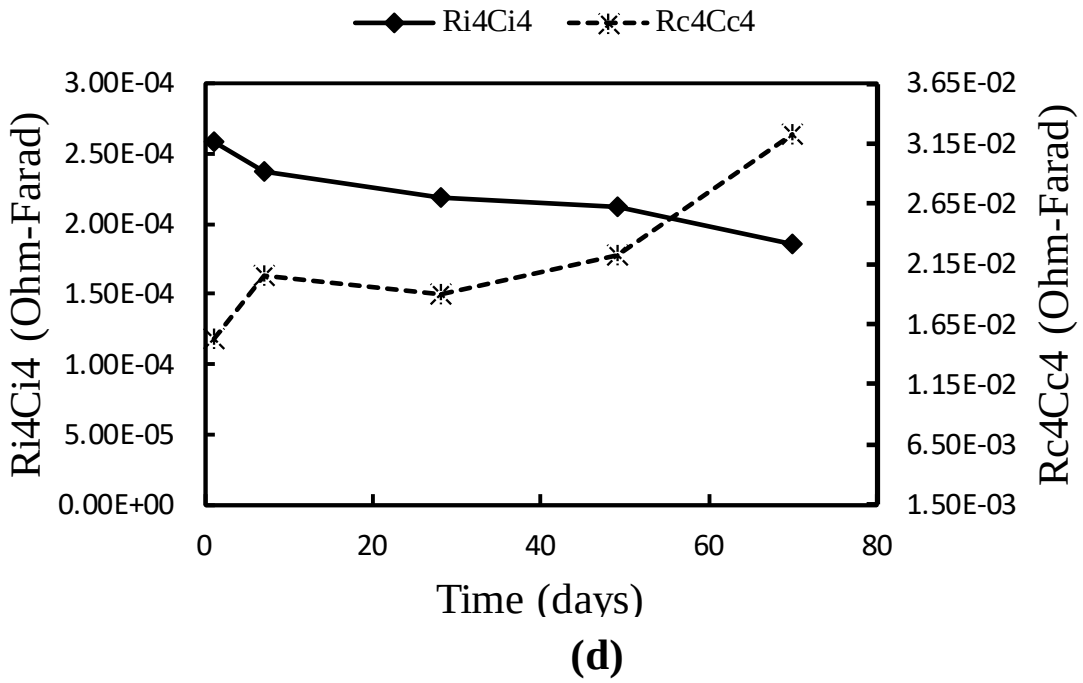

(d)

Figure 6-4 Change in (a) bulk resistance (Rb), (b) interface resistance (Ri) & contact resistance (Rc), (c) interface capacitance (Ci) & contact capacitance (Cc), and (d) corrosion index (RC) over time for M1-C4 configuration of moist sand specimen

Table 6-7 Model parameters of the equivalent circuit for M1-C4 configuration of the moist sand specimen

Days	Rb	Ri4	Ci4	Rc4	Cc4	Ri4Ci4	Rc4Cc4	R^2	RMSE
1	1714.5	229.9	1.12E-06	1198.0	1.27E-05	2.59E-04	1.52E-02	0.9862	19.32
7	1868.0	245.1	9.71E-07	1764.0	1.16E-05	2.38E-04	2.05E-02	0.9448	31.24
28	1888.0	284.9	7.67E-07	1808.5	1.05E-05	2.18E-04	1.90E-02	0.9527	41.68
49	1902.9	376.8	5.63E-07	2214.0	1.00E-05	2.12E-04	2.22E-02	0.9101	47.51
70	2030.3	440.8	4.20E-07	3363.5	9.60E-06	1.85E-04	3.23E-02	0.9586	33.18

Table 6-8 Change in model parameters for M1-C4 configuration of the moist sand specimen

Days	Change in Rb	Change in Ri4	Change in Ci4	Change in Rc4	Change in Cc4	Change in Ri4Ci4	Change in Rc4Cc4
7	8.96%	6.60%	-13.64%	47.25%	-8.73%	-7.94%	34.38%
28	10.12%	23.93%	-31.81%	50.96%	-17.26%	-15.50%	24.90%
49	10.99%	63.91%	-49.95%	84.81%	-21.30%	-17.97%	45.45%
70	18.42%	91.72%	-62.62%	180.76%	-24.57%	-28.33%	111.77%

6.2.1 Change in Bulk Resistance

The changes in the bulk resistance (Rb) for M1-C1, M1-C2, M1-C3, and M1-C4 configurations are shown in Figures 6-1, 6-2, 6-3, and 6-4, respectively. Although resistance is not a material property, the percentage change in resistance is directly related to the percentage change in resistivity. The bulk resistance for the M1-C1 configuration increased from 37678.2 Ω to 41284.83 Ω over 70 days. For M1-C2 configuration Rb increased from 2226.37 Ω to 2639.11 Ω. For M1-C3 configuration Rb increased from 18204.5 Ω to 50491.93 Ω. For M1-C4 configuration Rb increased from 1714.46 Ω to 2030.3 Ω.

6.2.2 Change in Interface Resistance and Contact Resistance

The changes in the interface resistance (Ri) and contact resistance (Rc) for M1-C1, M1-C2, M1-C3, and M1-C4 configurations are shown in Figures 6-1, 6-2, 6-3, and 6-4, respectively. The interface resistance (Ri) for (1) M1-C1 configuration increased from 3402.63 Ω to 41284.83 Ω, (2) M1-C2 configuration increased from 375.95 Ω to 579.15 Ω, (3) M1-C3 configuration increased from 3467.5 Ω to 14769.76 Ω, and (4) M1-C4 configuration increased from 229.9 Ω to 440.8 Ω. The contact resistance (Rc) for (1) M1-C1 and M1-C3 configuration increased from

12045.78 Ω to 37615.5 Ω, and (2) M1-C2 and M1-C4 configuration increased from 1198 Ω to 3363.5 Ω.

6.2.3 Change in Interface Capacitance and Contact Capacitance

The changes in the interface capacitance (Ci) and contact capacitance (Cc) for M1-C1, M1-C2, M1-C3, and M1-C4 configurations are shown in Figures 6-1, 6-2, 6-3, and 6-4, respectively. The interface capacitance (Ci) for (1) M1-C1 configuration decreased from 7.95E-10 F to 2.91 E-11 F, (2) M1-C2 configuration decreased from 6.77E-07 F to 4.07E-07 F, (3) M1-C3 configuration decreased from 8.02E-08 F to 3.12E-09 F, and (4) M1-C4 configuration decreased from 1.12E-06 F to 4.2E-07 F. The contact capacitance (Cc) for (1) M1-C1 configuration decreased from 6.97E-07 F to 7.10E-08 F, and (2) M1-C2 configuration decreased from 1.43E-05 F to 6.97E-06 F, (3) for M1-C3 configuration decreased from 1.50E-06 F to 3.29E-07 F and (4) for M1-C4 configuration decreased from 1.27E-05 F to 9.60E-06 F.

6.2.4 Change in Electrical Corrosion Index

The electrical corrosion index which was defined as the product of resistance (R) and capacitance (C) was obtained for two cases: (1) the contacts of the wire probes with the moist sand which is represented as RcCc and (2) at the interface of the steel bar and moist sand which is represented as RiCi. Rc1Cc1 decreased from 8.40E-03 ΩF to 2.67E-03 ΩF. Rc2Cc2 increased from 1.72E-02 ΩF to 2.34E-02 ΩF. Rc3Cc3 decreased from 1.81E-02 ΩF to 1.24E-02 ΩF. Rc4Cc4 increased from 1.52E-02 ΩF to 3.23E-02 ΩF. The decrease in Rc1Cc1 and Rc3Cc3 values could be explained by the high percentage decrease in the value of contact capacitance Cc1 and Cc3 (~90% and ~78%, respectively). On the other hand, the increase in Rc2Cc2 and Rc4Cc4 can be seen as a result of a low percentage decrease in contact capacitance Cc2 and Cc4 (~51% and ~25%, respectively). Ri1Ci1 decreased from 2.71E-06 ΩF TO 1.20E-06 ΩF. Ri2Ci2 decreased from 2.55E-04 ΩF to 2.36E-04 ΩF. Ri3Ci3 decreased from 2.78E-04 ΩF to 4.61E-05 ΩF. Ri4Ci4 decreased from 2.59E-04 ΩF to 1.85E-04 ΩF. The RiCi values for all the configurations can be

seen to decrease as time goes on. This could be because of the relatively high percentage decrease in the value of interface capacitance in comparison to the percentage increase in interface resistance.

6.3 Corrosion Quantification of Steel Bar in Moist Clay

Like the previous study, the corrosion of steel bar in moist clay (40% moisture content by weight) was also studied. The impedance was measured using a commercial LCR device over a frequency range of 20 Hz to 300 kHz. The electrical impedance data was then collected and plotted as a function of the frequency. Like the above case, it was observed that the impedance curve corresponds to case 2 of the Vipulanandan Impedance Model, wherein the bulk material is represented by a resistor and the contacts are represented by a resistor and capacitor in parallel. The bulk resistance, contact resistance, and contact capacitance for the various probe configurations were computed by optimizing the model impedance data points in MS EXCEL program.

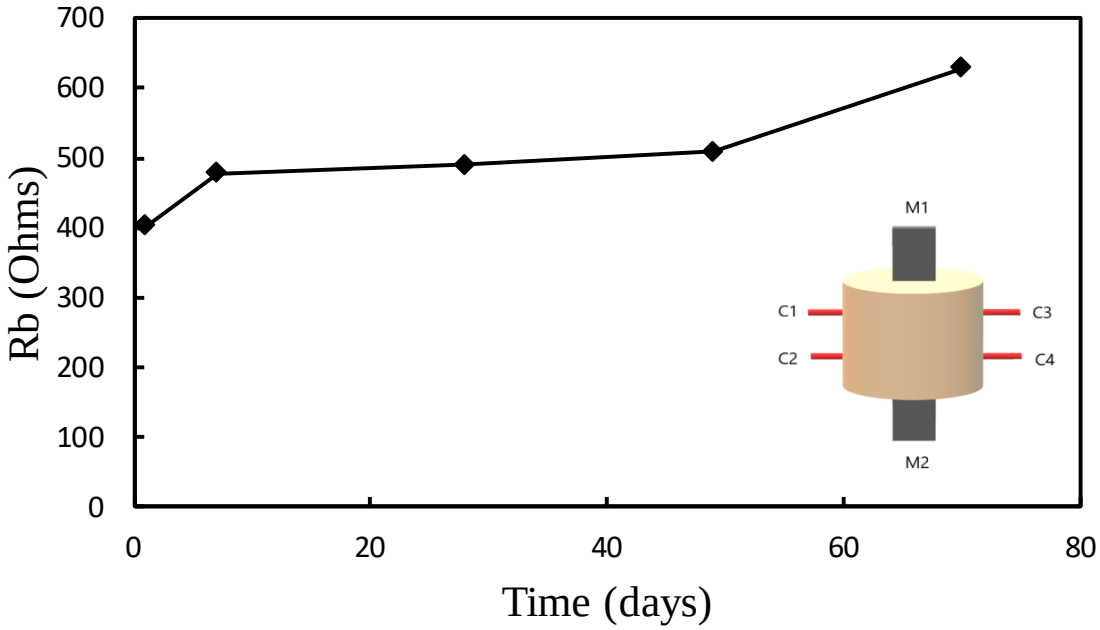
700
600
500
400
300
200
100
0
Rb (Ohms)
0
20
40
60
80
Time (days)
M1
C1
C3
C2
C4
M2

(a)

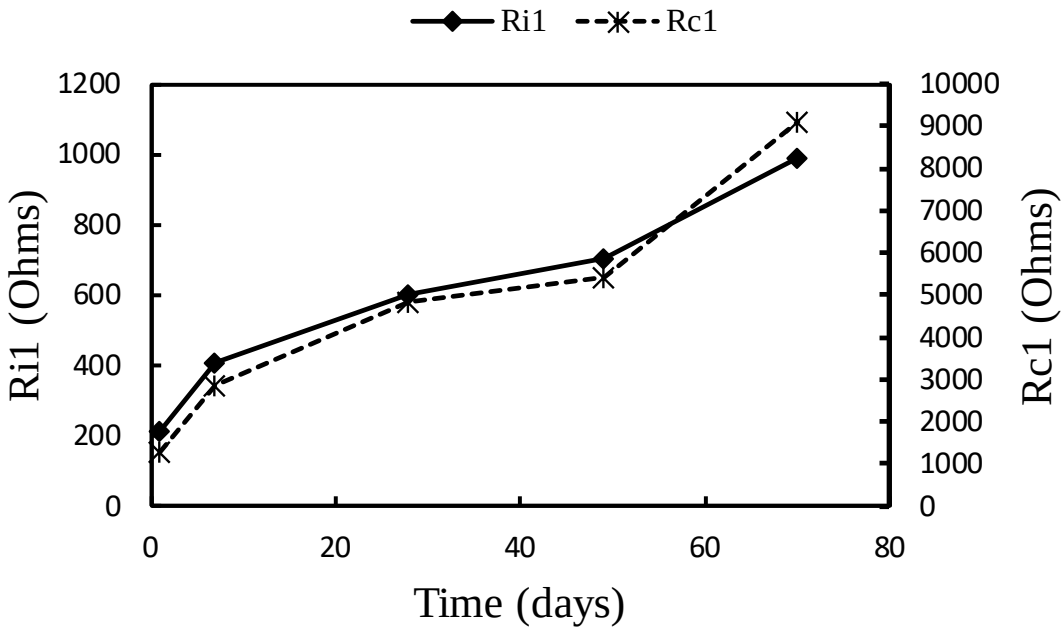
Ri1
Rc1
1200
1000
800
600
400
200
0
Ri1 (Ohms)
10000
9000
8000
7000
6000
5000
4000
3000
2000
1000
0
Rc1 (Ohms)
0
20
40
60
80
Time (days)

(b)

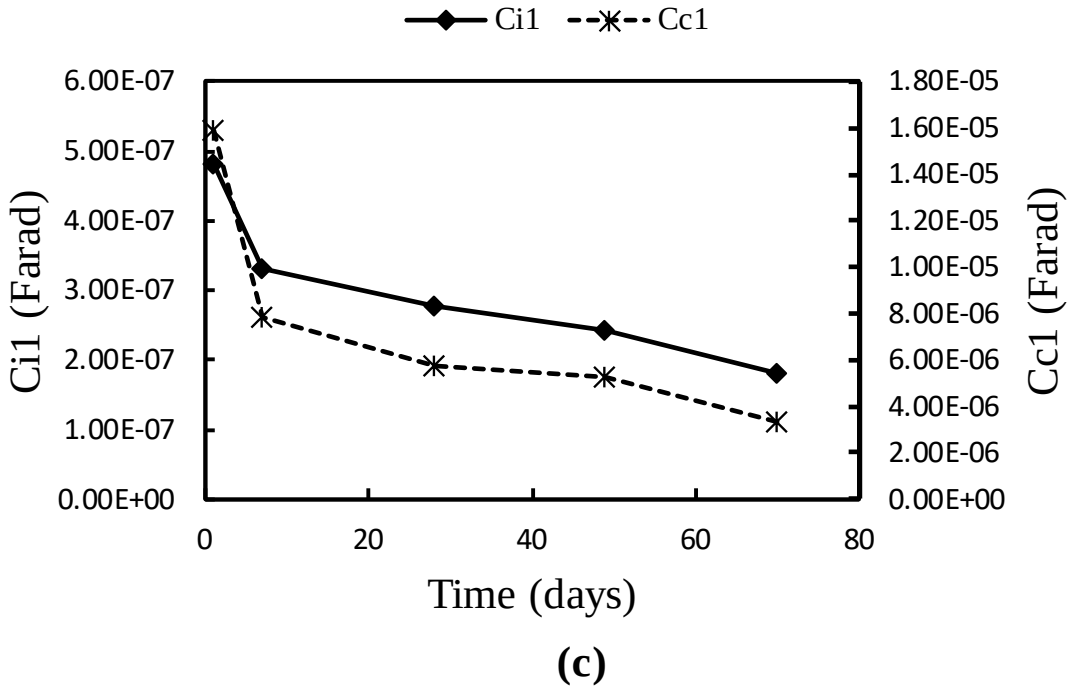

(c)

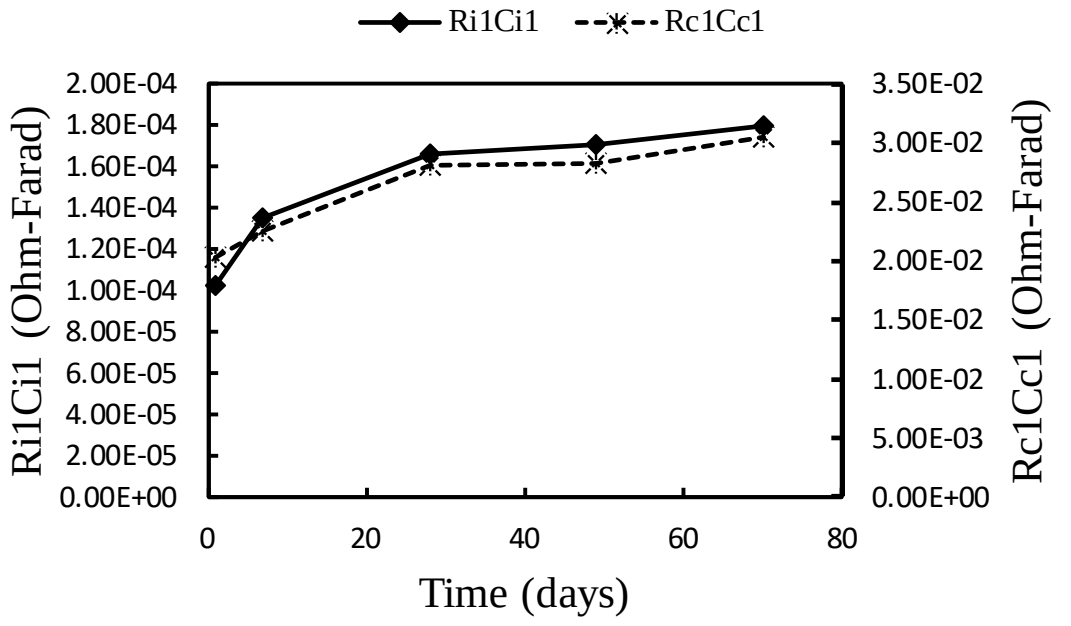

(d)

Figure 6-5 Change in (a) bulk resistance (Rb), (b) interface resistance (Ri) & contact resistance (Rc), (c) interface capacitance (Ci) & contact capacitance (Cc), and (d) corrosion index (RC) over time for M1-C1 configuration of moist clay specimen

Table 6-9 Model parameters of the equivalent circuit for M1-C4 configuration of the moist clay specimen

Days	Rb	Ri1	Ci1	Rc1	Cc1	Ri1Ci1	Rc1Cc1	R^2	RMSE
1	402.69	211.96	4.81E-07	1282.50	1.59E-05	1.02E-04	2.03E-02	0.9321	502.80
7	478.59	405.66	3.32E-07	2877.00	7.85E-06	1.35E-04	2.26E-02	0.8763	1262.03
28	489.41	599.64	2.78E-07	4857.50	5.78E-06	1.66E-04	2.81E-02	0.8821	2039.82
49	509.16	703.20	2.43E-07	5435.00	5.22E-06	1.71E-04	2.84E-02	0.9721	2791.92
70	628.11	990.40	1.81E-07	9094.01	3.36E-06	1.80E-04	3.05E-02	0.9649	3805.46

Table 6-10 Change in model parameters for M1-C1 configuration of the moist clay specimen

Days	Change in Rb	Change in Ri1	Change in Ci1	Change in Rc1	Change in Cc1	Change in Ri1Ci1	Change in Rc1Cc1
7	18.85%	91.39%	-30.98%	124.33%	-50.52%	32.10%	11.00%
28	21.53%	182.91%	-42.35%	278.75%	-63.56%	63.09%	38.03%
49	26.44%	231.76%	-49.47%	323.78%	-67.11%	67.65%	39.37%
70	55.98%	367.26%	-62.32%	609.08%	-78.84%	76.08%	50.07%

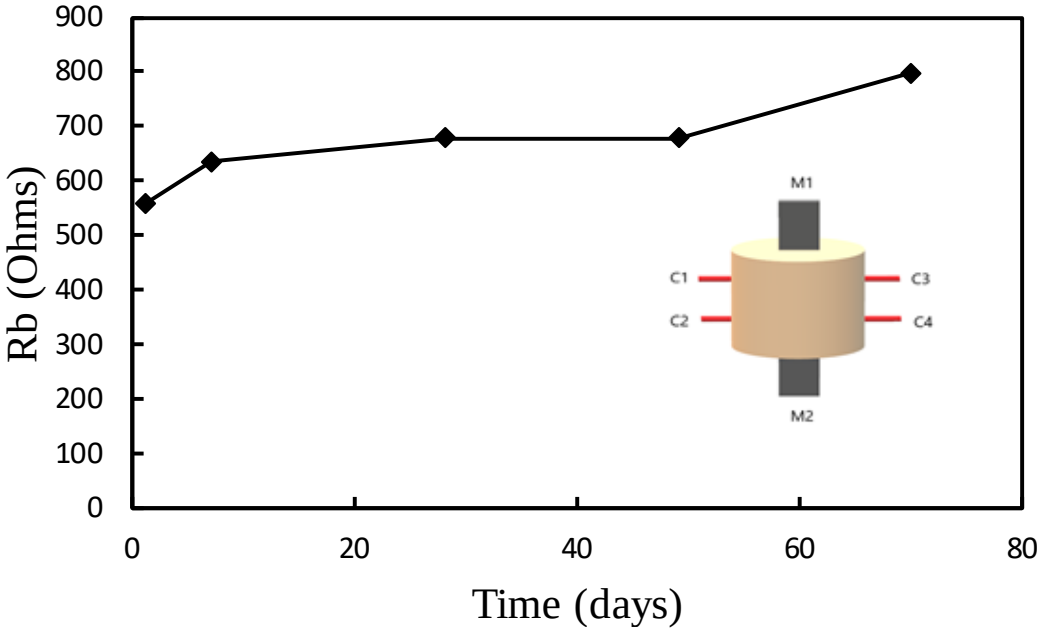
900
800
700
600
500
400
300
200
100
0
Rb (Ohms)
0
20
40
60
80
Time (days)
M1
C1
C3
C2
C4
M2

(a)

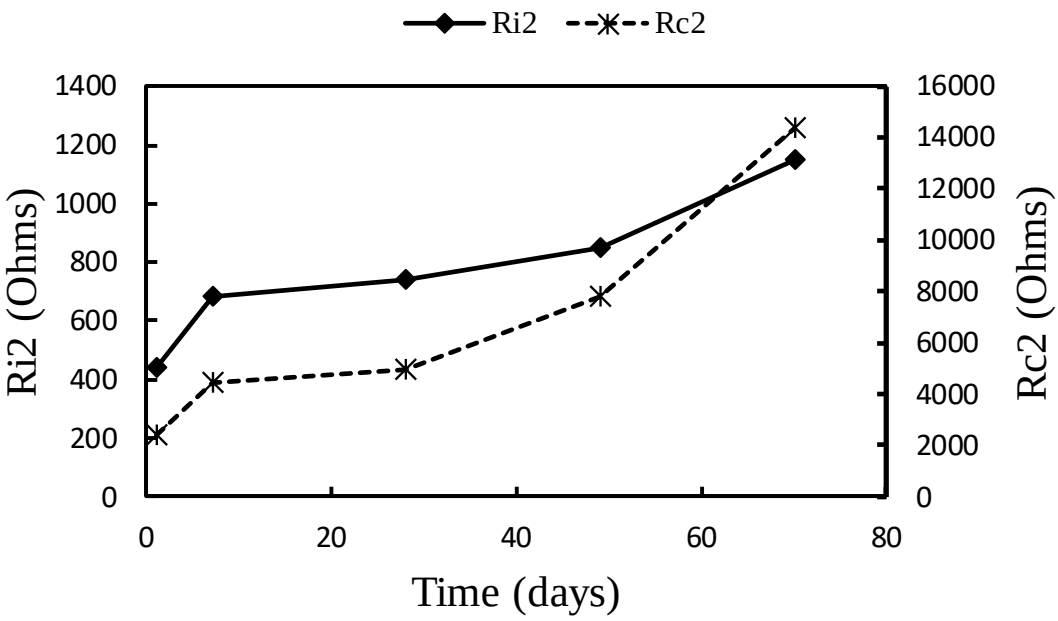
Ri2
Rc2
1400
1200
1000
800
600
400
200
0
Ri2 (Ohms)
16000
14000
12000
10000
8000
6000
4000
2000
0
Rc2 (Ohms)
0
20
40
60
80
Time (days)

(b)

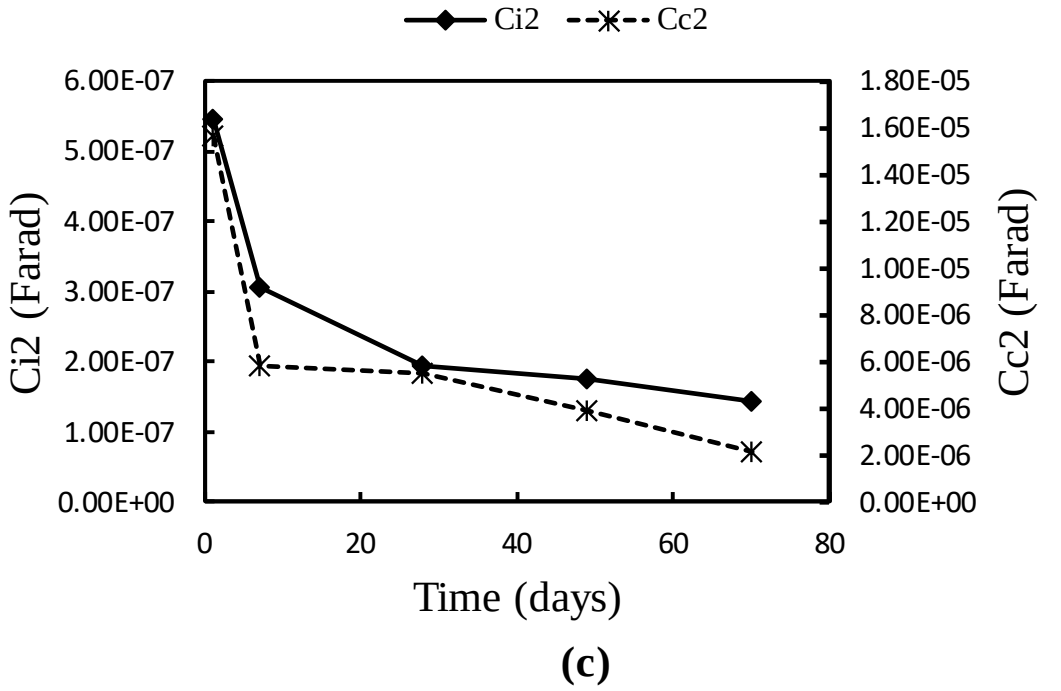

(c)

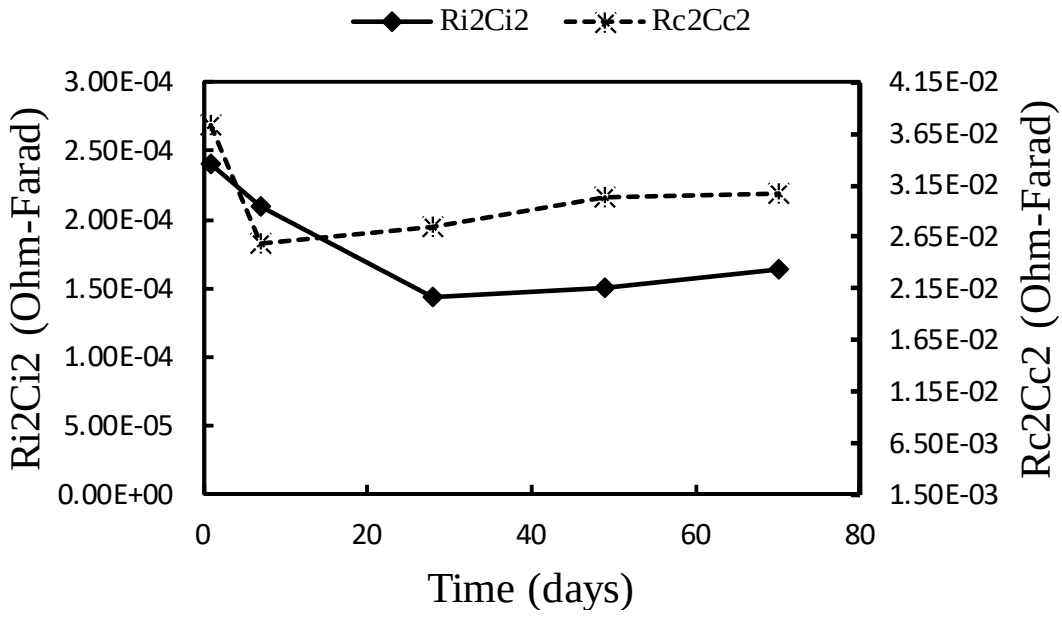

(d)

Figure 6-6 Change in (a) bulk resistance (Rb), (b) interface resistance (Ri) & contact resistance (Rc), (c) interface capacitance (Ci) & contact capacitance (Cc), and (d) corrosion index (RC) over time for M1-C2 configuration of moist clay specimen

Table 6-11 Model parameters of the equivalent circuit for M1-C2 configuration of the moist clay specimen

Days	Rb	Ri2	Ci2	Rc2	Cc2	Ri2Ci2	Rc2Cc2	R^2	RMSE
1	557.01	440.40	5.47E-07	2385.50	1.56E-05	2.41E-04	3.73E-02	0.9845	28.15
7	635.27	684.69	3.07E-07	4457.00	5.81E-06	2.10E-04	2.59E-02	0.9628	50.96
28	677.79	737.57	1.95E-07	4977.00	5.50E-06	1.44E-04	2.74E-02	0.9631	50.26
49	678.02	851.83	1.76E-07	7818.00	3.88E-06	1.50E-04	3.04E-02	0.9491	59.47
70	796.89	1146.26	1.43E-07	14383.99	2.14E-06	1.64E-04	3.07E-02	0.9571	46.49

Table 6-12 Change in model parameters for M1-C2 configuration of the moist clay specimen

Days	Change in Rb	Change in Ri2	Change in Ci2	Change in Rc2	Change in Cc2	Change in Ri2Ci2	Change in Rc2Cc2
7	14.05%	55.47%	-43.86%	86.84%	-62.87%	-12.73%	-30.63%
28	21.68%	67.48%	-64.28%	108.64%	-64.81%	-40.18%	-26.58%
49	21.72%	93.42%	-67.82%	227.73%	-75.16%	-37.76%	-18.60%
70	43.06%	160.28%	-73.91%	502.98%	-86.35%	-32.09%	-17.69%

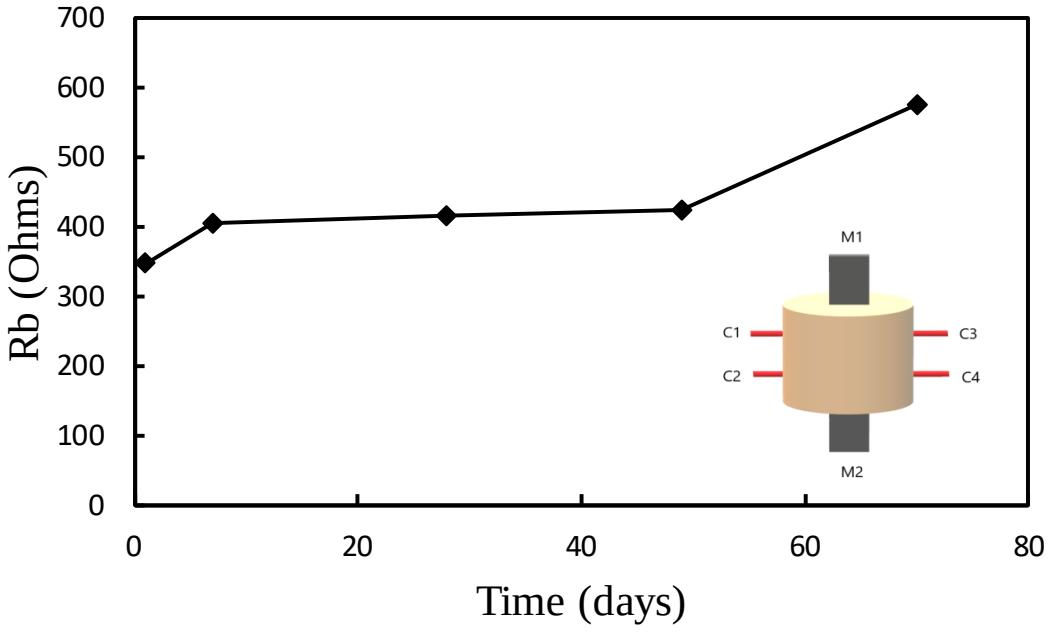
700
600
500
400
300
200
100
0
Rb (Ohms)
0
20
40
60
80
Time (days)
M1
C1
C2
C3
C4
M2

(a)

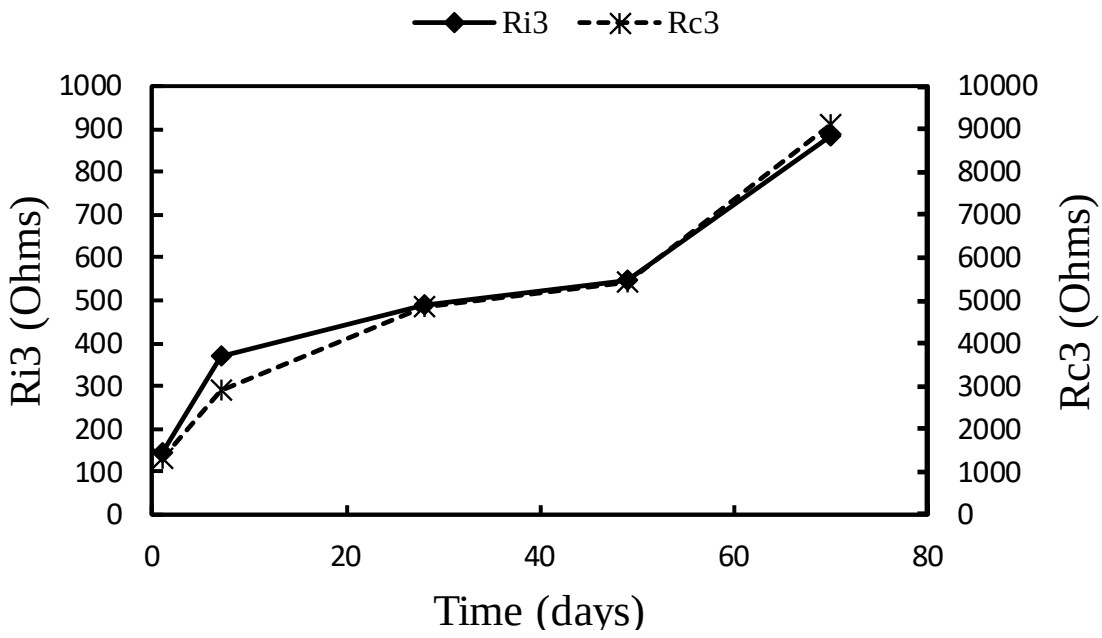
Ri3
Rc3
1000
900
800
700
600
500
400
300
200
100
0
Ri3 (Ohms)
10000
9000
8000
7000
6000
5000
4000
3000
2000
1000
0
Rc3 (Ohms)
0
20
40
60
80
Time (days)

(b)

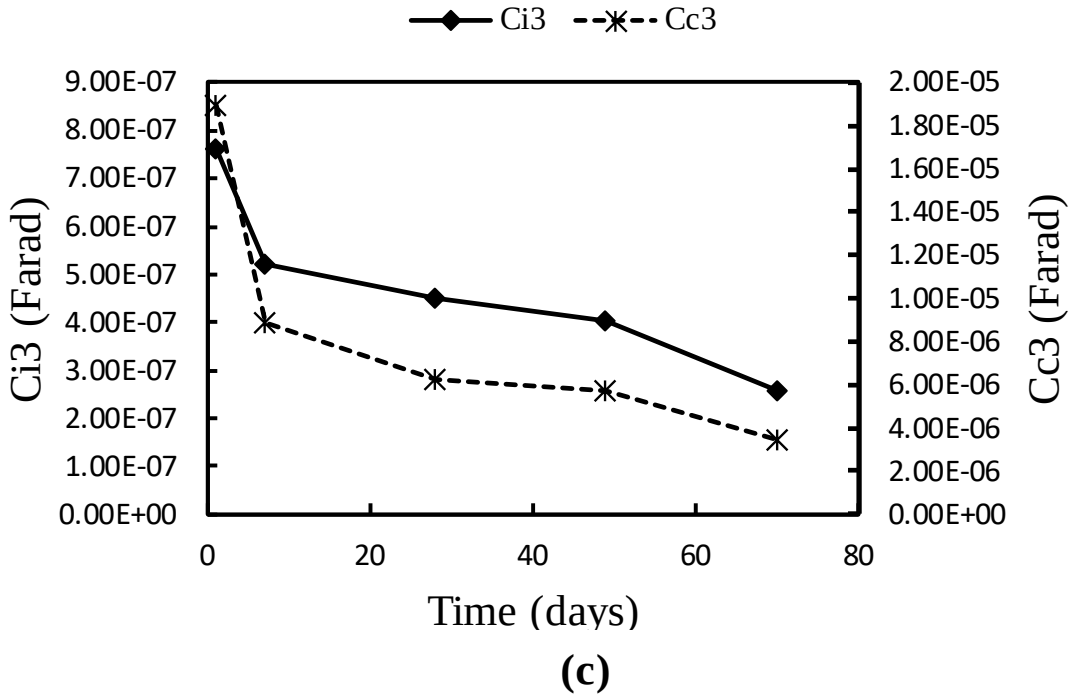

(c)

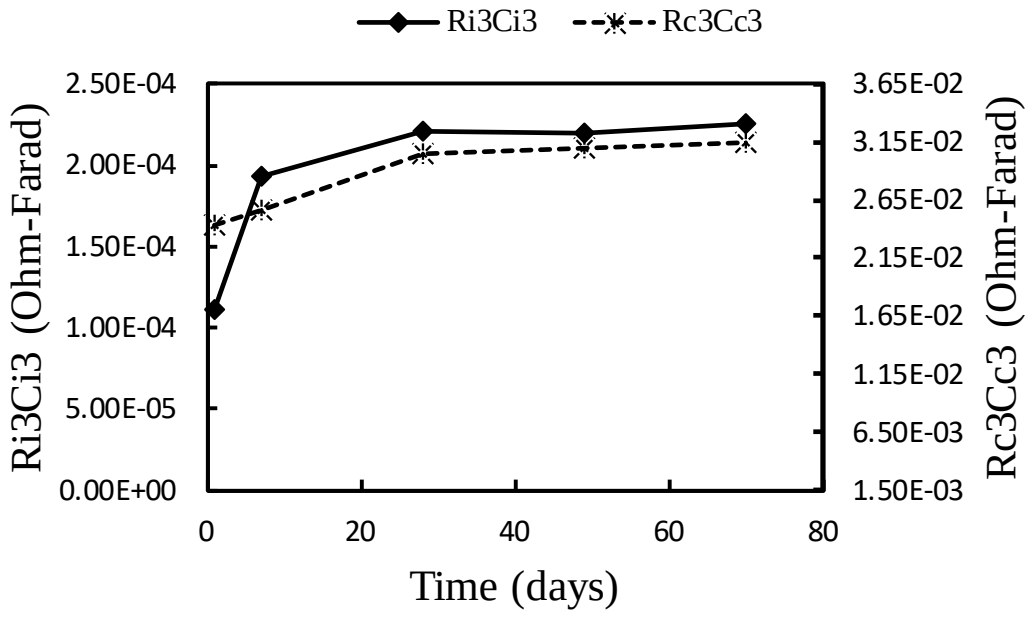

(d)

Figure 6-7 Change in (a) bulk resistance (Rb), (b) interface resistance (Ri) & contact resistance (Rc), (c) interface capacitance (Ci) & contact capacitance (Cc), and (d) corrosion index (RC) over time for M1-C3 configuration of moist clay specimen

Table 6-13 Model parameters of the equivalent circuit for M1-C3 configuration of the moist clay specimen

Days	Rb	Ri3	Ci3	Rc3	Cc3	Ri3Ci3	Rc3Cc3	R^2	RMSE
1	347.31	145.20	7.63E-07	1282.50	1.89E-05	1.11E-04	2.43E-02	0.9730	279.62
7	404.24	370.41	5.22E-07	2877.00	8.88E-06	1.93E-04	2.55E-02	0.9728	336.69
28	416.40	491.20	4.49E-07	4857.50	6.27E-06	2.20E-04	3.05E-02	0.9677	632.99
49	424.51	547.60	4.02E-07	5435.00	5.71E-06	2.20E-04	3.10E-02	0.9117	1840.58
70	575.52	882.19	2.55E-07	9093.99	3.45E-06	2.25E-04	3.14E-02	0.8335	2784.45

Table 6-14 Change in model parameters for M1-C3 configuration of the moist clay specimen

Days	Change in Rb	Change in Ri3	Change in Ci3	Change in Rc3	Change in Cc3	Change in Ri3Ci3	Change in Rc3Cc3
7	16.39%	155.11%	-31.56%	124.33%	-53.07%	74.60%	5.28%
28	19.89%	238.30%	-41.22%	278.75%	-66.85%	98.84%	25.56%
49	22.23%	277.14%	-47.32%	323.78%	-69.84%	98.69%	27.79%
70	65.71%	507.58%	-66.54%	609.08%	-81.75%	103.29%	29.44%

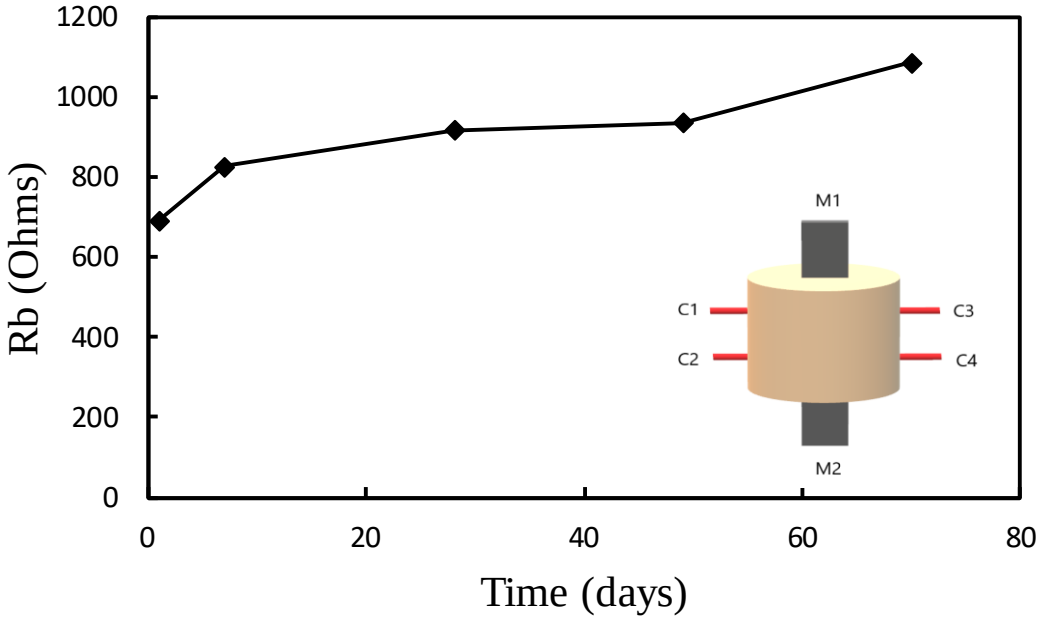
1200
1000
800
600
400
200
0
Rb (Ohms)
0
20
40
60
80
Time (days)
M1
C1
C3
C2
C4
M2

(a)

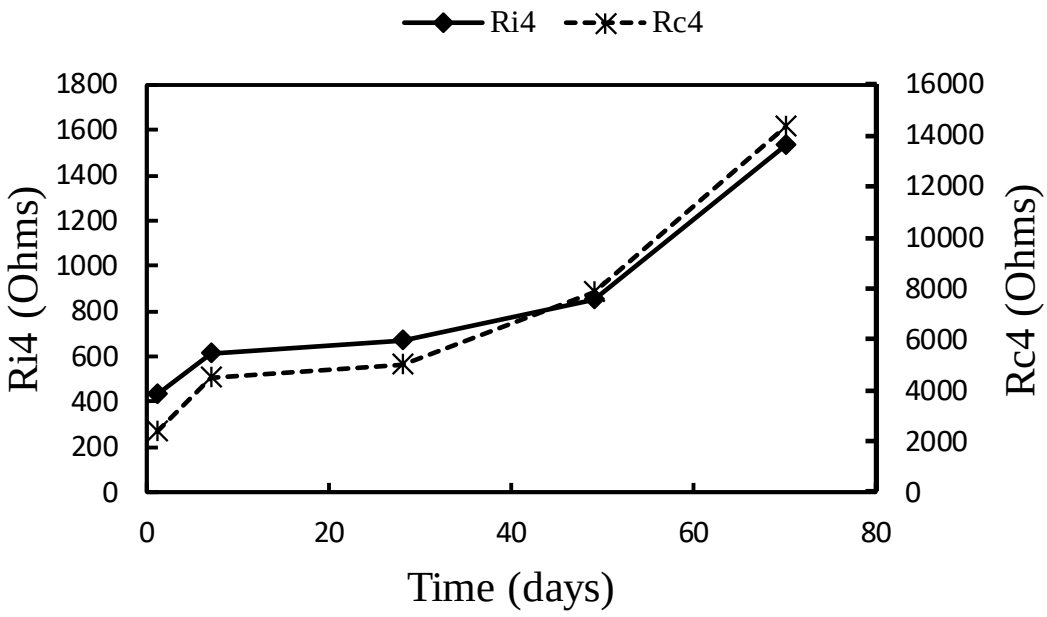
Ri4
Rc4
1800
1600
1400
1200
1000
800
600
400
200
0
Ri4 (Ohms)
16000
14000
12000
10000
8000
6000
4000
2000
0
Rc4 (Ohms)
0
20
40
60
80
Time (days)

(b)

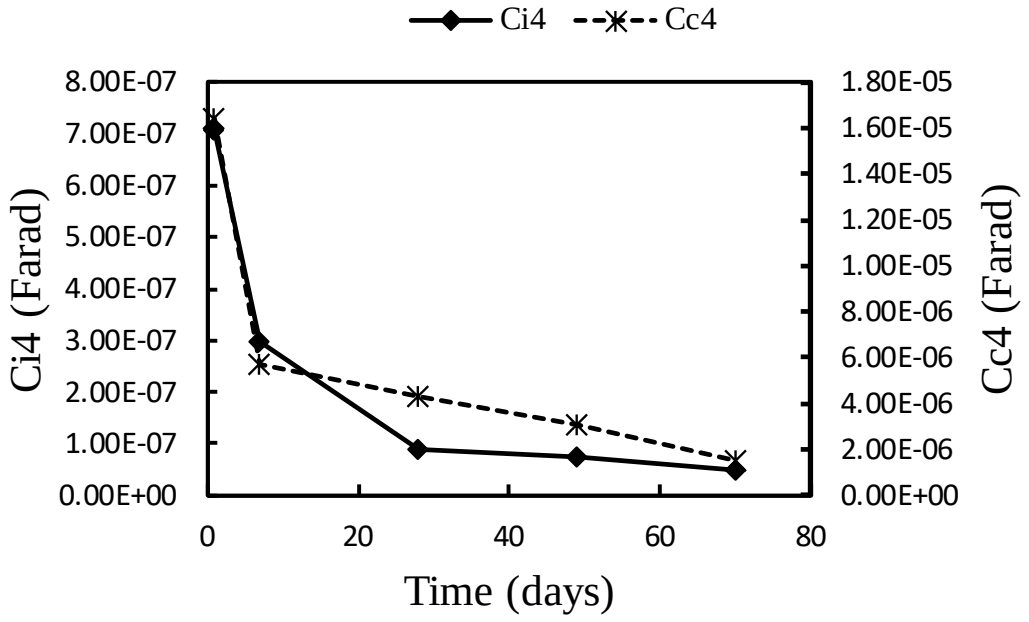

(c)

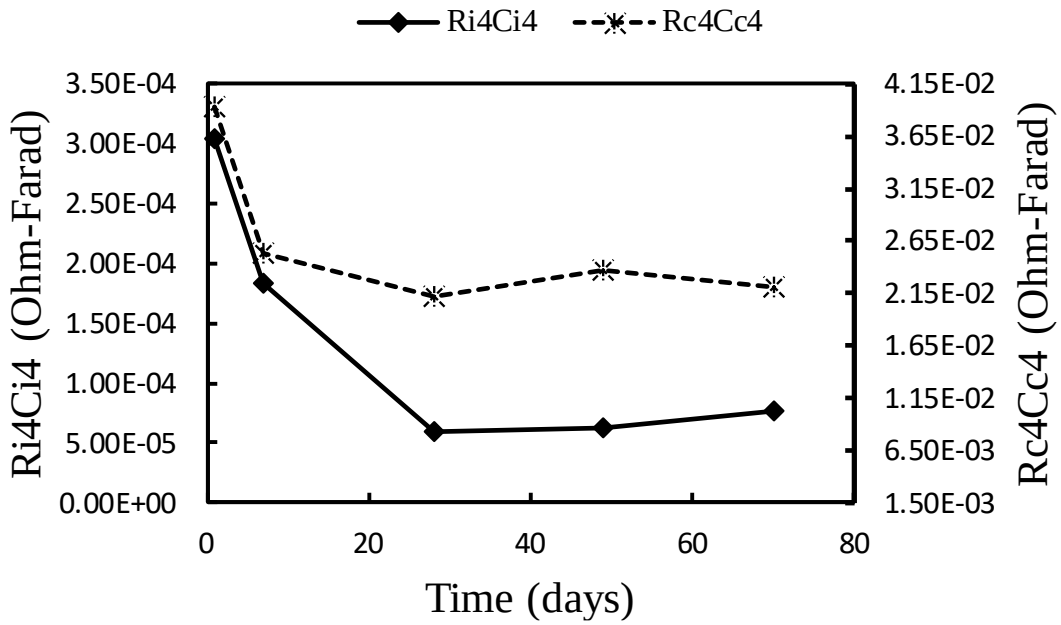

(d)

Figure 6-8 Change in (a) bulk resistance (Rb), (b) interface resistance (Ri) & contact resistance (Rc), (c) interface capacitance (Ci) & contact capacitance (Cc), and (d) corrosion index (RC) over time for M1-C4 configuration of moist clay specimen

Table 6-15 Model parameters of the equivalent circuit for M1-C4 configuration of the moist clay specimen

Days	Rb	Ri4	Ci4	Rc4	Cc4	Ri4Ci4	Rc4Cc4	R^2	RMSE
1	692.4	428.9	7.10E-07	2385.5	1.64E-05	3.04E-04	3.92E-02	0.9862	19.32
7	828.2	615.4	2.98E-07	4457.0	5.67E-06	1.83E-04	2.53E-02	0.9448	31.24
28	917.9	672.9	8.87E-08	4977.0	4.26E-06	5.97E-05	2.12E-02	0.9527	41.68
49	936.6	852.0	7.26E-08	7818.0	3.04E-06	6.19E-05	2.38E-02	0.9101	47.51
70	1088.5	1534.4	4.95E-08	14384.0	1.53E-06	7.60E-05	2.20E-02	0.9586	33.18

Table 6-16 Change in model parameters for M1-C4 configuration of the moist clay specimen

Days	Change in Rb	Change in Ri4	Change in Ci4	Change in Rc4	Change in Cc4	Change in Ri4Ci4	Change in Rc4Cc4
7	19.61%	43.46%	-58.00%	86.84%	-65.55%	-39.75%	-35.63%
28	32.58%	56.88%	-87.50%	108.64%	-74.09%	-80.40%	-45.94%
49	35.27%	98.63%	-89.77%	227.73%	-81.52%	-79.68%	-39.45%
70	57.21%	257.71%	-93.02%	502.98%	-90.69%	-75.04%	-43.84%

6.3.1 Change in Bulk Resistance

The changes in the bulk resistance (Rb) for M1-C1, M1-C2, M1-C3, and M1-C4 configurations are shown in Figures 6-5, 6-6, 6-7, and 6-8, respectively. The bulk resistance for the M1-C1 configuration increased from 402.69 Ω to 628.11 Ω over 70 days. For M1-C2 configuration Rb increased from 557.01 Ω to 796.89 Ω. For M1-C3 configuration Rb increased from 347.31 Ω to 575.52 Ω. For M1-C4 configuration Rb increased from 692.4 Ω to 1088.5 Ω.

6.3.2 Change in Interface Resistance and Contact Resistance

The changes in the interface resistance (Ri) and contact resistance (Rc) for M1-C1, M1-C2, M1-C3, and M1-C4 configurations are shown in Figures 6-5, 6-6, 6-7, and 6-8, respectively. The interface resistance (Ri) for (1) M1-C1 configuration increased from 211.96 Ω to 990.4 Ω, (2) M1-C2 configuration increased from 440.4 Ω to 1146.26 Ω, (3) M1-C3 configuration increased from 145.2 Ω to 882.19 Ω, and (4) M1-C4 configuration increased from 428.9 Ω to 1534.4 Ω. The contact resistance (Rc) for (1) M1-C1 and M1-C3 configuration increased from 1282.5 Ω to 9094.01 Ω, and (2) M1-C2 and M1-C4 configuration increased from 2385.5 Ω to 14384 Ω.

6.3.3 Change in Interface Capacitance and Contact Capacitance

The changes in the interface capacitance (Ci) and contact capacitance (Cc) for M1-C1, M1-C2, M1-C3, and M1-C4 configurations are shown in Figures 6-5, 6-6, 6-7, and 6-8, respectively. The interface capacitance (Ci) for (1) M1-C1 configuration decreased from 4.81E-07 F to 1.81E-07 F, (2) M1-C2 configuration decreased from 5.47E-07 F to 1.43E-07 F, (3) M1-C3 configuration decreased from 7.63E-07 F to 2.55E-07 F, and (4) M1-C4 configuration decreased from 7.10E-07 F to 4.95E-08 F. The contact capacitance (Cc) for (1) M1-C1 configuration decreased from 1.59E-05 F to 3.36E-06 F, and (2) M1-C2 configuration decreased from 1.56E-05 F to 2.14E-06 F, (3) for M1-C3 configuration decreased from 1.89E-05 F to 3.45E-06 F and (4) for M1-C4 configuration decreased from 1.64E-05 F to 1.53E-06 F.

6.3.4 Change in Electrical Corrosion Index

The electrical corrosion index (product of R and C) was obtained for two cases: (1) the contacts of the wire probes with the moist clay which is represented as RcCc and (2) at the interface of the steel bar and moist clay which is represented as RiCi. Rc1Cc1 increased from 2.03E-02 ΩF to 3.05E-02 ΩF. Rc2Cc2 decreased from 3.73E-02 ΩF to 3.07E-02 ΩF. Rc3Cc3 increased from 2.43E-02 ΩF to 3.14E-02 ΩF. Rc4Cc4 decreased from 3.92E-02 ΩF to 2.20E-02 ΩF. The increase in Rc1Cc1 and Rc3Cc3 values could be explained by the relatively low percentage decrease in the value of contact capacitance Cc1 and Cc3 (~79% and ~82%, respectively) as opposed to the percentage increase in contact resistance Rc1 and Rc3 (~609%). On the other hand, the decrease in Rc2Cc2 and Rc4Cc4 can be seen as a result of the relatively high percentage decrease in contact capacitance Cc2 and Cc4 (~86% and ~91%, respectively) as opposed to the percentage increase in contact resistance Rc2 and Rc4 (~503%). Ri1Ci1 increased from 1.02E-04 ΩF TO 1.80E-04 ΩF. Ri2Ci2 decreased from 2.41E-04 ΩF to 1.64E-04 ΩF. Ri3Ci3 increased from 1.11E-04 ΩF to 2.25E-04 ΩF. Ri4Ci4 decreased from 3.04E-04 ΩF to 7.60E-05 ΩF. The RiCi values for M1-C1 and M1-C3 configurations can be seen to increase as time goes on while for configurations M1-C2

and M1-C4 it can be seen to decrease over the same period of days. The increasing trend of the Ri1Ci1 and Ri3Ci3 could be because of the relatively low percentage decrease in interface capacitance Ci1 and Ci3 (~62% and ~67%, respectively) as opposed to the percentage increase in interface resistance Ri1 and Ri3 (~367% and ~507%, respectively). The decreasing trend of the Ri2Ci2 and Ri4Ci4 could be because of the relatively high percentage decrease in interface capacitance Ci2 and Ci4 (~74% and ~93%, respectively) as opposed to the percentage increase in interface resistance Ri2 and Ri4 (~160% and ~258%, respectively).

6.4 Comparison of Steel Corrosion in Cement and Soil

The electrical impedance method shows the corrosion kinetics and evolution of corrosion over time in the different corrosion specimens. The interface resistance of the cement-steel casing showed an increase in almost 8 times its initial value in the 250 days period and roughly 3 times in 70 days period. The interface resistance of the (1) steel bar in moist sand showed an increase in almost 2 times its initial value while (2) in moist clay it showed an increase in almost 3.5 times in the 70 days period. The corrosion index at the interface of the cement-steel casing for combination M-C4 decreased from 1.44E-04 ΩF to 1.50E-05 ΩF in 250 days which translates to a decrease of 94.24%. The corrosion index at the interface of the steel bar in 10% moist sand for combination M1-C4 decreased from 2.59E-04 ΩF to 1.85E-04 ΩF in 70 days which translates to a decrease of 24.57%. In comparison, the corrosion index at the interface of the steel bar in 40% moist clay for combination M1-C4 decreased from 3.04E-04 ΩF to 7.60E-05 ΩF in the same 70 days period which translates to a decrease of 90.69%.

6.5 Summary

In this study the corrosion behavior of a steel bar in two different soil types: sand and clay with different moisture content was studied and modeled using the Vipulanandan Impedance Model. Based on the experimental results the following conclusions can be drawn:

1. The steel bar was allowed to corrode in moist sand and clay for 70 days. To measure the impedance measurements of the sample, a commercial LCR device was used. The electrical resistance readings obtained for the various wire probe configurations of the cement-steel casing showed that the specimen corresponded to Case 2 of the Vipulanandan Impedance Model.
2. In the moist sand specimen, the interface resistance increased 3402.63 Ω to 41284.83 Ω for M-C1 configuration, 375.95 Ω to 579.15 Ω for M-C2 configuration, 3467.5 Ω to 14769.76 Ω for M-C3 configuration, and m 229.9 Ω to 440.8 Ω for M-C4 configuration. In the moist clay specimen, the interface resistance increased from 211.96 Ω to 990.4 Ω for M-C1 configuration, 440.4 Ω to 1146.26 Ω for M-C2 configuration, 145.2 Ω to 882.19 Ω for M-C3 configuration, 428.9 Ω to 1534.4 Ω and M-C4 configuration. This increase in the interface resistance suggests that corrosion is occurring at the interface of the steel bar and moist soil.
3. The interface corrosion index RiCi for all the wire probe configurations of the moist sand saw a decrease in its value over the 70 days. This behavior of RiCi could be a result of the high percentage decrease in the interface capacitance value (Ci) in comparison to the percentage increase in interface resistance value (Ri).
4. In the case of moist clay, the interface corrosion index RiCi for M1-C1 and M1-C3 configurations saw an increase in their value over time while for M1-C2 and M1-C4 configurations it saw a decrease in the value over the same period. The increasing trend of Ri1Ci1 and Ri3Ci3 could be because of the relatively low percentage decrease in interface capacitance Ci1 and Ci3 (~62% and ~67%, respectively) as opposed to the percentage increase in interface resistance Ri1 and Ri3 (~367% and ~507%, respectively) while the decreasing trend of Ri2Ci2 and Ri4Ci4 could be because of the relatively high percentage decrease in interface capacitance Ci2 and Ci4 (~74% and

~93%, respectively) as opposed to the percentage increase in interface resistance Ri2 and Ri4 (~160% and ~258%, respectively).

CHAPTER 7 CONCLUSIONS

Based on this study the following conclusions are advanced:

1. From the study of the effect of moisture content on the electrical resistivity of soil, it was proven that the resistivity of the two soil types taken: Ottawa sand and bentonite clay is dependent on the amount of the permeating fluid, the porosity, and pore continuity of the sand specimen. Thus, the resistivity value drops for higher water content and after saturation, the value remains constant.
2. The impedance data collected for both the soil types indicated that impedance decreased with increasing frequency and became constant after reaching 300 kHz. This behavior shown by the two soil types signifies that the bulk resistance of the material influences its impedance value. Hence, it follows case 2 of the Vipulanandan Impedance Model.
3. Resistivity as a function of moisture content for the two soil types was successfully modeled using the Hyperbolic function and Exponential function.
4. The electrical impedance method shows the corrosion kinetics and evolution of corrosion over time in the different corrosion specimens. The electrical impedance model circuit proposed by Vipulanandan can be an effective method to predict the corrosion occurring at the interface of the steel specimen.

REFERENCES

Arriba-Rodriguez, L. D., Villanueva-Balsera, J., Ortega-Fernandez, F., & Rodriguez-Perez, F. (2018). Methods to Evaluate Corrosion in Buried Steel Structures: A Review. *Metals*, *8*(5), 334. https://doi.org/10.3390/met8050334

Corrosion: Understanding the Basics (March 19, 2000). (2021). Asm Intl (March 19, 2000).

Doyle, G., Seica, M. V., & Grabinsky, M. W. (2003). The role of soil in the external corrosion of cast iron water mains in Toronto, Canada. *Canadian Geotechnical Journal*, *40*(2), 225–236. https://doi.org/10.1139/t02-106

Ekine, A., & Emujakporue, G. (2010). Investigation of Corrosion of Buried Oil Pipeline by the Electrical Geophysical Methods. *Journal of Applied Sciences and Environmental Management*, *14*(1). https://doi.org/10.4314/jasem.v14i1.56492

Ezuber, H. M., Alshater, A., Hossain, S. M. Z., & El-Basir, A. (2020). Impact of Soil Characteristics and Moisture Content on the Corrosion of Underground Steel Pipelines. *Arabian Journal for Science and Engineering*, *46*(7), 6177–6188. https://doi.org/10.1007/s13369-020-04887-8

Gupta, S., & Gupta, B. (1979). The critical soil moisture content in the underground corrosion of mild steel. *Corrosion Science*, *19*(3), 171–178. https://doi.org/10.1016/0010-938x(79)90015-5

Ismail, A., & Elshamy, A. (2009). Engineering behaviour of soil materials on the corrosion of mild steel. *Applied Clay Science*, *42*(3–4), 356–362. https://doi.org/10.1016/j.clay.2008.03.003

Lim, K. S., Yahaya, N., Othman, S. R., Fariza, S., & Noor, N. (2013). The Relationship between Soil Resistivity and Corrosion Growth in Tropical Region. *The Journal of Corrosion Science and Engineering*, *16*. https://www.researchgate.net/publication/270310264_The_Relationship_between_Soil_Resistivity_and_Corrosion_Growth_in_Tropical_Region

Mazumder, J. M. A. (2020, June 2). *Global Impact of Corrosion: Occurrence, Cost and Mitigation*. Iris Publishers. https://irispublishers.com/gjes/fulltext/global-impact-of-corrosion-occurrence-cost-and-mitigation.ID.000618.php

McNeil, J. D. (1980). Electrical Conductivity of Soils and Rocks. *Geonics LTD.* Published.

Noor, E. A., & Al-Moubaraki, A. H. (2014). Influence of Soil Moisture Content on the Corrosion Behavior of X60 Steel in Different Soils. *Arabian Journal for Science and Engineering*, *39*(7), 5421–5435. https://doi.org/10.1007/s13369-014-1135-2

Penhale, H. R. (1958). Corrosion of mild steel in some New Zealand soils. *New Zealand Journal of Science*, *1*(1), 52–69. https://doi.org/10.7931/DL1-SBP-0134

Rajani, B., & Makar, J. (2000). A methodology to estimate remaining service life of grey cast iron water mains. *Canadian Journal of Civil Engineering*, *27*(6), 1259–1272. https://doi.org/10.1139/l00-073

Romanoff, M. (1957). Underground Corrosion. *National Bureau of Standards Circular 579; National Bureau of Standards: Washington, DC, USA*

Schütze, M. (2002). Corrosion Books: Handbook of Corrosion Engineering. By Pierre R. Roberge - Materials and Corrosion 4/2002. *Materials and Corrosion*, *53*(4), 284.

Secer, M., & Uzun, E. T. (2017). Corrosion Damage Analysis of Steel Frames Considering Lateral Torsional Buckling. *Procedia Engineering*, *171*, 1234–1241. https://doi.org/10.1016/j.proeng.2017.01.415

Song, Y., Jiang, G., Chen, Y., Zhao, P., & Tian, Y. (2017). Effects of chloride ions on corrosion of ductile iron and carbon steel in soil environments. *Scientific Reports*, *7*(1). https://doi.org/10.1038/s41598-017-07245-1

Veleva, L. (1996). Soils and Corrosion. In R. Baboian (Ed.), *Corrosion Tests and Standards: Application and Interpretation* (2nd ed., pp. 387–404). ASTM International.

Vipulanandan, C., & Chockalingam, C. (2018). Steel Corrosion Detection and Quantification Real-Time Using the New Nondestructive Test with Vipulanandan Impedance Corrosion Model. *American Association of Drilling Engineers*. Published.